Development and Application of a Non Invasive Image Matching Method to Study Spine Biomechanics

by

Shaobai Wang

B.S., Mechanical Engineering
University of Michigan, 2006

Submitted to the Department of Mechanical Engineering
in partial fulfillment of the requirements for the degree of
Master of Science in Mechanical Engineering
at the

MASSACHUSETTS INSTITUTE OF TECHNOLOGY

June 2008

Signature of Author.....
Department of Mechanical Engineering
May 12, 2006

Certified by.....
Guoan Li
Associate Professor of Orthopaedic Surgery
Harvard Medical School
Thesis Supervisor

Accepted by.....
Lallit Anand
Professor of Mechanical Engineering
Chairman, Committee on Graduate Students

Development and Application of a Non Invasive Image Matching Method to Study Spine Biomechanics

by

Shaobai Wang

Submitted to the Department of Mechanical Engineering
on May 15, 2008 in partial fulfillment of the
requirements for the degree of
Master of Science in Mechanical Engineering

Abstract

Research on spine biomechanics is critical to understand pathology such as degenerative changes and low back pain. However, current study on in-vivo spine biomechanics is limited by the complex anatomy and invasive methodology. Modern clinical imaging techniques such as magnetic resonance and fluoroscope images, which are widely accessible nowadays, have the potential to study in-vivo spine biomechanics accurately and non-invasively. This research presents a new combined magnetic resonance and fluoroscope imaging matching method to study human lumbar vertebral kinematics and disc deformation during various physiologic functional activities. Validation and application of this method as well as discussion of its performance and applicability are detailed herein.

Thesis Supervisor: Guoan Li

Title: Associate Professor of Orthopaedic Surgery

Harvard Medical School

Acknowledgment

I have to admit the acknowledgment is my favorite part and this is my first time to write one. Maybe not many people will get a chance to read this. However, I'd like to say, I don't know how to put this but I'm kind of a big deal. First and foremost I thank my mom Du Chen and dad Wang Hui Lian. At this age and after three years living by myself, I now fully understand how much they care for me and love me. I have tons of words to say to them and I'll tell them personally instead of write here since they don't understand English and I would rather make them proud and take good care of them to show the love. My sister Wang Ya Nan and my cousin Ding Guo Hao has also supported me throughout my life and made my world more interesting.

I must also thank the many teachers and mentors of me, who enriched me with knowledge as well as the philosophy of life. Dr. Guoan Li introduced me to this research and he's both a nice supervisor and a good friend.

Finally I'd like to acknowledge my lots of friends in China and in the United States. If I should list all the names and fun times, it will definitely overwhelm the main part of the thesis. So don't feel that I forgot you, and as far as we share the best memories, we are always best friends. Jeffery Bingham is one coolest guy among all. George Hanson is one peppiest guy among all. I'd like to use two words I learned from them to show my respect, shenanigan and punk. I won't ever forget the great time we had. I wish both of you success in your school work and love.

I'd like to end with an old Chinese saying, "*sān gè chòu pí jiàng, sài guò zhū gě liàng*". This saying translates as "three stinky leatherworkers (leatherheads?) surpass the greatest legendary military counselor (*zhū gě liàng*) in the Three Kingdoms era". I'm not saying that I'm stinky or silly. I mean with the help from all the people, I finished the research, I will achieve success and I will live happily ever.

Contents

List of Figures

List of Tables

List of Abbreviations

Low Back Pain (LBP)

Degenerative Disc Disease (DDD)

Three Dimensional (3D)

Two Dimensional (2D)

Magnetic Resonance Imaging (MRI)

Computer Tomography (CT)

Dual Orthogonal Fluoroscopic ImageS (DFIS)

Six Degree-Of-Freedom (6DOF)

Range Of Motion (ROM)

Finite Rlement Models (FEM)

Motion Segment Unit (MSU)

Intervertebral disc (IVD)

Annulus Fibrosus (AF)

Nucleus Pulposus (NP)

Total Disc Replacement (TDR)

Standard Deviation (SD)

3 Tesla (3T)

Iterative Closest Point (ICP)

Institutional Review Board (IRB)

Digital Imaging and Communications in Medicine (DICOM)

Chapter 1

Introduction

Low back pain (LBP) secondary to degenerative changes in the lumbar spine is thought to be multi-factorial in etiology [1,2]. It has been reported that 75% of all adults will experience LBP secondary to degenerative disc disease (DDD) in the lumbar spine at some point in their lifetime [3,4]. Even though various biological and biomechanical reasons have been proposed, no quantitative data has been reported to describe the mechanisms of this degeneration. Altered vertebral kinematics has been assumed to be a critical factor leading to this development. Understanding of the biomechanical mechanisms of spinal diseases requires a clear definition of kinematics of vertebra as well as intervertebral disc (IVD) deformation. However, due to the complex anatomy and limited technology, there is currently no published study that has investigated the biomechanics of the vertebral kinematics and disc deformation under physiologic functional activities in the lumbar spine.

A newly developed, non-invasive magnetic resonance imaging (MRI) combined and dual orthogonal fluoroscopic imaging system (DFIS) technique will be used to quantify the in-vivo lumbar spine biomechanics. Three dimensional (3D) MRI models of the lumbar spine segments will be matched to the two dimensional (2D) features of the acquired fluoroscopic images in the two perpendicular views during different physiologic functional activities to study vertebral kinematics and disc deformation.

The technique differs from traditional 2D-3D registration techniques that

were designed to determine target joint motion. With the DFIS technique, dynamic positions of the target joint are captured in two orthogonal directions and the joint position is determined simultaneously using the dual image sets and the 3D models. This technique has been extensively validated in terms of its accuracy and repeatability for determining in-vivo human joint position and cartilage deformation [5-11]. Recently, a thorough validation of this method for the lumbar spine has been accepted for publication in the Journal of Spine [12]. Our previous studies using this technique have contributed greatly to the understanding of kinematics of human joints, both native as well as joints that have sustained degenerative changes, traumatic injuries, and joints that have undergone reconstructive surgical procedures [6,7,10,13,14].

The development and application of combined MRI and DFIS is presented in this thesis for the purpose of study in-vivo spine biomechanics. Accuracy and repeatability of the technique to determine six degree-of-freedom (6DOF) translation and rotation of the spine are discussed. In-vivo vertebral kinematics and disc deformation from normal subjects under various physiologic functional activities are studied.

1.1 Previous studies in spine biomechanics

1.1.1 In-vitro spine biomechanics study

Numerous studies have been carried out using in-vitro experimental setups to investigate the biomechanics of the spine [15-26]. The main advantage of in-vitro methods is the comprehensive visualization of joint function with respect to the individual anatomy. For example, Goel et al. [27] reported on spine mechanics during normal, injured and stabilized conditions. Ketter et al. [20] indicated that the

finite helical axes of motion are useful tools to describe the three dimensional in-vitro kinematics of the intact and stabilized spine. Miura and Panjabi et al. [21] studied the in-vitro flexibility of C2-T1 specimens under compressive preloading. Fujiwara et al. [28] conducted an in vitro anatomic and biomechanical study using human cadaveric lumbar spines. They evaluated the changes in the intervertebral foramen during flexion and extension, lateral bending, and axial rotation of the lumbar spine and correlated these changes with the flexibility of the spinal motion segments by imaging the spine before and after the application of rotational and loading movements. After all these studies used invasive techniques to obtain their measurements which add morbidity when applied to an in-vivo setting. In addition, these studies have the obvious disadvantage of being performed in-vitro which makes them difficult to interpret in the clinical setting. Finally, the objective measurements obtained are not directly clinically relevant.

1.1.2 In-vitro disc deformation study

IVD deformation is a complex physiologic behavior that has contributory biological, biochemical and biomechanical components which have been studied. In-vitro studies intend to investigate the problem from different aspects, yet limitations exist from the in-vitro nature of these research. **Biological models** employ a variety of cell, tissue, or organ culture techniques [29-31] with culture conditions that partially mimic the cellular environment of the human IVD. Mechanical loading has been incorporated into the model to study the interaction between biomechanics and biology [32-36]. It has not yet been determined, however, whether cultured cells can be clinically used to regenerate a damaged IVD.

Biomechanical models include IVD or motion segment unit (MSU) loading experiments such as axial loading, moments and combinations. Disc properties and behaviors, such as modulus [37,38], disc creep [39,40], disc shear [41,42],

intradisc pressure [43-45] and disc bulging [46,47] were studied using pressure and displacement transducers. Experimental studies have also attempted to measure internal disc deformation using radiographic or optical imaging methods by introducing metal beads, thin wires or physically tracking markers [48-52]. Other researchers studied the biomechanical characteristics of discs after removal of the nucleus pulposus (NP) or after chemonucleolysis to simulate degenerative changes [53-57]. However, these loading experiments are facing challenging of intra-specimen variability, difficulty in including muscle activity, and inability to mimic fluid exchange of the disc.

Finite element models (FEM) have been applied to understand the relationships between the biomechanical performance of the disc and disc degeneration. Nonlinearity of the material and geometry has been considered in the model [58-60]. Viscoelasticity and fiber-reinforced annulus fibrosus (AF) was introduced [61-63]. Recently, a popular poroelastic material behavior has been introduced to FEM to consider fluid flow of the disc [64-68]. Regional poroelastic material properties and strain-dependent permeability and porosity has also been investigated [69,70]. The FEM introduces lots of parameters to describe the disc prosperity. The validities of these values require carefully examination. On the other hand, although rudimental validation studies incorporating animal models, in-vitro tests and artificial hydrogel disc model have been carried out [66,71], the relevance of the FEM IVD model to in-vivo IVD deformation remains a challenge.

Animal models such as rats, rabbits, dogs and primates have been described in literature in an attempt to provide these models with clinical relevance. Despite the ethic concerns, the cost-efficient and clinical relevance to human beings still need to be further investigated.

1.1.3 In-vivo spine biomechanics study

To better understand the in-vivo spine biomechanics, methods that aim to minimize the invasion while maintain acceptable accuracy appear by taking advantages of advanced medical image techniques. **CT imaging technique** has been widely used for spine kinematics research [16,24,72-78] Among these studies, Ochia et al. [79] attempted to examine in-vivo lumbar spinal segmental motion using parallel CT scans [80]. Fifteen asymptomatic volunteers underwent three separate CT scans at different positions (supine and left and right rotations). They used these images to construct separate three-dimensional models, and then calculated segmental motions using Euler angles and volume merge methods in three major planes. The data revealed that spinal torsion resulted in complex coupled motions in the lumbar spinal segments. However, CT scans expose subjects to large amounts of ionizing radiation that is particularly concerning when imaging is performed for isolated research purposes. In addition, although this technique does provide kinematics data in various positions of the spine it does not do so under conditions of physiological loading.

MR imaging has also been applied extensively for the study of spinal kinematics and has several attractive attributes [81-96]. McGregor, et al. [97] used interventional open MRI to assess the kinematics of the lumbar spine in patients with spondylolisthesis. The findings were compared with those in a published database of subjects with no history of LBP. Kulig et al. [91] assessed lumbar spine kinematics using dynamic MRI in 2004. In their study, a proposed mechanism of sagittal plane motion was induced by manual posterior-to-anterior mobilization. Siddiqui et al. [16] studied twenty-six patients with lumbar spinal stenosis to understand the in-vivo sagittal kinematics of the lumbar spine at the instrumented and adjacent levels. Pre- and postoperative positional MRI were conducted in the

standing, supine, and sitting positions in both flexion and extension. Measurements of disc heights, endplate angles, segmental and lumbar range of motion were performed and a significant difference was found. Vitzthum et al. [98] also conducted a study that determined the relationship of different structures of the lower lumbar spine during interventional movement examination by MRI methods. While MRI imaging has minimum radiation, MRI limitations include prolonged scanning times during which patient must keep still and inadequacy in describing kinematics in 3D space.

Fluoroscopic and conventional X-ray techniques have been used in various studies on spinal kinematics [15,17,99]. Auerbach et al. [15] evaluated the spinal kinematics following lumbar total disc replacement (TDR) and circumferential fusion using in-vivo fluoroscopy. Wong et al. [17] designed the video-fluoroscopy system with a new auto-tracking technique for the continuous assessment of lumbar spine kinematics. Intervertebral flexion and extension (L1-L5) were assessed in 30 healthy volunteers. Allen et al. [99] examined spinal kinematics using video-fluoroscopy imaging combined with digital image processing. The parameters studied were instantaneous centers of rotation, intervertebral angles, angles of rotation and displacement for each vertebral joint. Harvey et al. [100] measured lumbar spinal flexion-extension kinematics from lateral radiographs, simulating the effects of out-of-plane movements and errors in the placement of reference points. These studies are able to capture spine kinematics in 2D, however the information is missing for out of plane motion and the errors are comparably big.

Electromagnetic motion measurement devices have also been used in spine research [101-108]. McGregor et al. [102] aimed to quantify rowing technique in terms of lumbopelvic motion, force production, and work done at different work

intensities. The electromagnetic motion measuring device in conjunction with a load cell was used to determine the ergometer rowing kinematics of 12 elite international oarswomen during a routine step test. Steffen [105] measured lumbar spinal kinematics using 6 DOF electromagnetic tracking system (FASTRAK, Polhemus, USA). Burnett et al. [103] presented a pilot study to examine whether differences existed in spinal kinematics and trunk muscle activity in cyclists with and without non-specific chronic LBP. Spinal kinematics was measured by an electromagnetic tracking system and EMG was recorded bilaterally from selected trunk muscles. Holt et al. [104] developed a system using an electromagnetic motion system and strain gauge instrumented load cell to measure spinal and pelvic motion and force generated at the handle during rowing on an exercise rowing ergometer. He revealed marked increases in the amount of spinal segmental motion during the hour piece. The relevance of this with regard to LBP requires further investigation.

1.1.4 In-vivo disc deformation study

In-vivo human research attempts have primarily concentrated on the measurement of strain and the evaluation of nuclear migration using imaging technique. Most of these studies are limited in 2D. Using **MRI,** Brault et al. positioned 10 healthy male in MRI machines with supporting pad under the back at flexion and extension [109]. Brault et al. analyzed the pixel intensity along the horizontal mid-discal transect MRI slices and obtained an equation to mathematically curve-fit the intensity profile to study nucleus pulposus (NP) migration during flexion and extension. Fazey et al. took T2 MRI scan of three asymptomatic female subjects in flexed, extended, and left rotated positions combined with flexion and extension [84]. They employed a pixel profile technique to determine direction and magnitude of nuclear deformation. Recently,

O'Connell studied in-vitro disc strains non-invasively in axial compression using MRI [110]. MR images were acquired before and during application of a 1000 N axial compression. Two-dimensional internal displacements, average strains, and the location and direction of peak strains were calculated using texture correlation, a pattern matching algorithm. They studied height loss, disc bulging and strains.

Ultrasound has also been used to study in-vivo disc deformation [111]. In-vivo creep of human lumbar motion segments and discs subject to pure tension was studied. Elongation of segments was measured by a computerized subaqual ultrasound measuring method as a change of the distance between two adjacent spinous processes. From time-related measured elongation values, in-vivo damping constants with creep functions were calculated for each segment, in terms of sex, aging and disc level.

1.2 Motivation

The above literature review demonstrates that spine kinematics and disc deformation have been investigated extensively using various techniques. Collectively, these studies have dramatically improved our understanding of spinal biomechanics and disc deformation and have helped to improve the surgical treatment of spinal degeneration. However, despite these advances, a quantitative understanding of kinematics and IVD deformation in the human spine under in-vivo physiologic functional activities remains elusive. There is little data that has been reported on either in-vivo 6DOF kinematics or 3D disc deformation under in-vivo physiologic functional activities. Knowledge of spine biomechanics in normal subjects is critical for the understanding of the mechanisms of spinal degeneration as well as for the further improvement of surgical techniques designed to restore normal spine kinematics. Due to the complex anatomy and

loading conditions, a quantitative investigation of in-vivo human spine disc deformation presents challenge to the current biomedical engineering technologies.

The MRI combined DFIS image matching method can be applied to most of the articulating joint in the human body. This allows for highly accurate in-vivo study of joint kinematics, dynamics, cartilage contact and ligament interaction. This non-invasive imaging technique should provide important information on the intrinsic biomechanics of the human spine. Using this technique, the research will be a first attempt to study kinematics and disc deformation in normal subjects under in-vivo physiologic functional activities. It will provide baseline information of the relationship between abnormal in-vivo biomechanics and the mechanisms of spinal degeneration. The knowledge obtained from this study will help to establish guidelines for the improvement of current surgical techniques and implant design for the treatment of patients with varying degrees of DDD, as well as provide objective functions for the development of tissue engineered biomaterials for disc degeneration repair.

Chapter 2

Image Matching Method on Spine Study

The concept of image matching is relatively simple. A 3D model is obtained through advanced medical image techniques such as MRI and CT. The fluoroscopic images of the subject in various physical functional activities are taken. Based on the perpendicular geometry of dual fluoroscopes setup, the 6DOF position and orientation of the 3D model can be quantitatively determined from excessive 2D features in radiographs. When model and features are matched, the kinematics is recreated. Due to its non-invasive manner and effectiveness on studying complex geometry, this image matching method can be applied on spine study.

2.1 Imaging

With the technological advancements in medical imaging such as magnetic resonance imaging (MRI), computer tomography (CT) and x-ray machines, it is possible to recreate fully 3D anatomical models and also record human physiologic activities in real time. MRI and CT provide tools to recreate the anatomy with sub-millimeter precision. Even though both the CT and MR models had similar accuracy, there is one inherent benefit of using CT imaging for the application of our technique. CT images may facilitate automatic segmentation with commercially available software. In contrast, automatic segmentation for MR models is currently time consuming. However, when measuring vertebral kinematics in human subjects, the dosage of radiation to which the subjects are exposed when utilizing CT imaging may present an ethical concern for the safety

of the individuals being tested. Alternatively, MR model provide us with greater visualization of the ligamentous components surrounding the lumbar vertebra as well as their relation to relevant neurologic structures in this area. Compare to the above two imaging technique, x-ray has the advantage of recreating real time 2D perspective image of the region of interest and patients are not restricted in prone or supine position as in MRI or CT. Thus this part explored MRI, CT for vertebral segment model generation and pulsed fluoroscopy for acquiring images of patient motion.

2.1.1 MRI

In order to create anatomic 3D model of lumbar spine, MRI has been utilized. Patients are asked to lie supine in a 3 Tesla (3T) MRI machine (MAGNETOM Trio, Siemens, Germany). Using a spine surface coil and a T2 weighted fat suppressed 3D SPGR sequence, parallel sagittal images with a thickness of 1mm without gap, and with a resolution of 512 x 512 pixels were obtained. A field of view of 180×180 mm is able to capture the whole lumbar vertebral segment from level L1 to L5. (**Fig. 2-1**)

Figure 2-1: An example MRI slice of the human lumbar spine from L1 to L5 in the sagittal plane for the purpose to build 3D anatomic model.

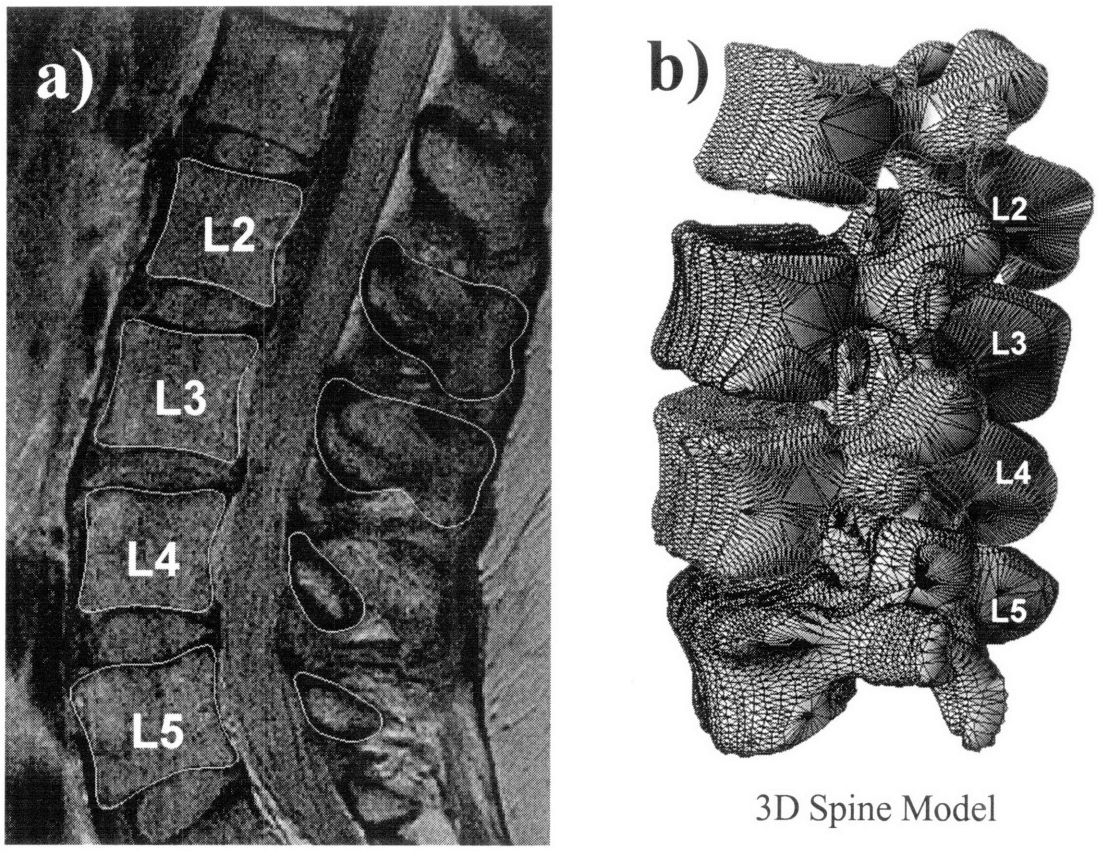

Figure 2-2: a) Contours of the vertebrae bodies was digitized with spline curves give the anatomy information of the lumbar spine. b) 3D mesh model can be generated from digitized contours of MRI layer by layer.

The MR images of the lumbar spine were then imported into a solid modeling software Rhinoceros® (Robert McNeel & Associates, Seattle, WA)to construct a 3D anatomical model of the segments using a protocol established in our laboratory [112]. The contours of the vertebrae bodies were digitized manually based on image intensity using B-Spline curves (**Fig. 2-2a**). The contour lines were then output into Rhinoceros to construct a 3D anatomical mesh model of the segments. An example of the digitization and mesh is shown in (**Fig. 2-2b**).

2.1.2 CT

The spine model can also be obtained from CT scanner (LightSpeed Pro16, GE, Waukesha, WI) using high-resolution axial plane images in the supine position. Images were obtained with a thickness of 0.625 mm and a gap of 0.625 mm, and with a resolution of 512 x 512 pixels. The CT images of the spinal segment were then imported into Matlab® (the MathWorks, Natick, MA). Based on the gradient of image intensity caused by bony structures, Canny edge detection algorithm has been utilized to automatically segment the vertebral bodies [113]. The algorithm first smooths the image using a Gaussian filter, and then it computes the gradients from a Laplacian filter. Next, the gradients are reduced by removing non-maximal values. The edges created by the maximal values are further reduced by applying a threshold and examining connectivity. Non-maximal edges connected to maximal edges are kept, while isolated non-maximal edges are removed. Canny edge detection is implemented in Matlab. An example of segmentation is in **Fig. 2-3a**.

Due to the complex geometry of most anatomical structures and the inherent lack of an edge in biological images, the outlines from the edge detection are manually reviewed. Manual editing is specially implemented at facet joint and at between proximal and distal segments attaches as there are decrease in intensity gradient. 3D anatomical mesh models of the vertebrae were then created from the digitized data. (**Fig. 2-3b**)

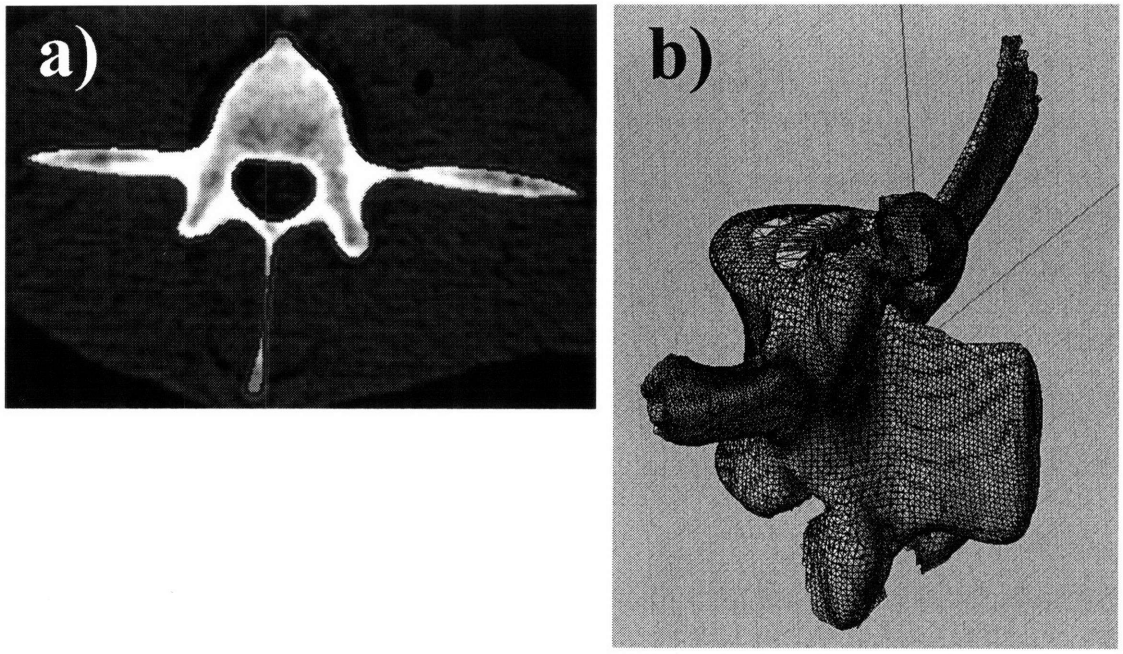

Figure 2-3: a) Automatic segmentation based on canny edge detection for spine CT scan. b) 3D mesh model constructed from the digitized data.

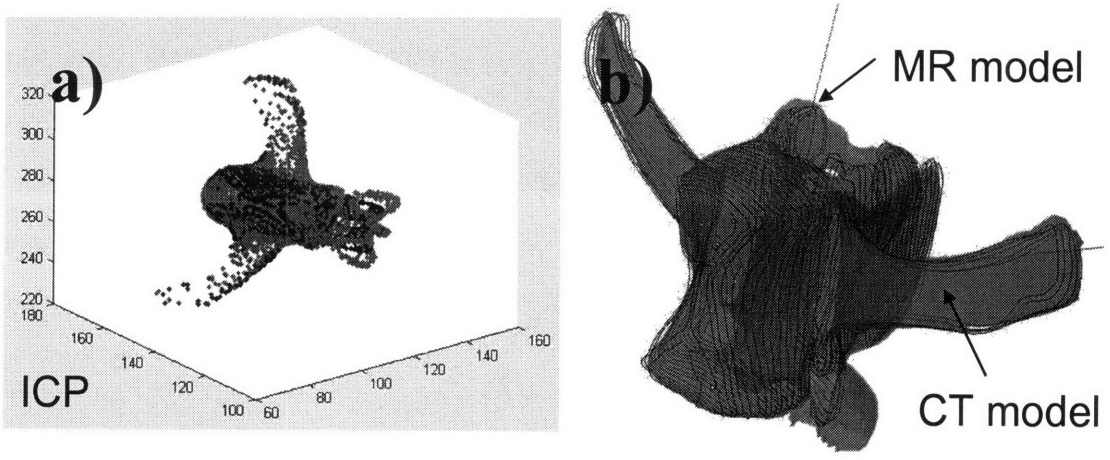

Figure 2-4: a) Iterative closest point algorism registers the MRI model with CT model. b) Comparison suggests satisfying geometric agreement with subtle differences.

2.1.3 MRI and CT model registration

Since CT models have been widely used by researchers to study spine kinematics [16,24,72-79] and CT model is generated from automatic segmentation based on Canny edge detection, we employed it as a comparison with MR models. The constructed CT and MR image-based models were then mapped together using a customized code implemented in the Matlab based on the iterative closest point (ICP) method [114]. About 4000 points were picked from both vertebral body models. The determination of the optimal shape matching of the two models was characterized by a convergence criterion that using changes in directional derivative of the matching process [114]. The average difference between the two mesh models was calculated to be 0.07±1.1 mm when mapping MR model to CT model. (**Fig. 2-4**)

2.1.4 Dual orthogonal fluoroscopic

The dual orthogonal fluoroscopic imaging system (DFIS) consists of two fluoroscopes (BV Pulsera, Philips, Netherlands) positioned perpendicular to each other. A subject is free to move within the common imaging zone of the two fluoroscopes. The system is capable to capture real time images of the spine segments simultaneously. A demonstration of the DFIS is shown in **Fig. 2-5**.

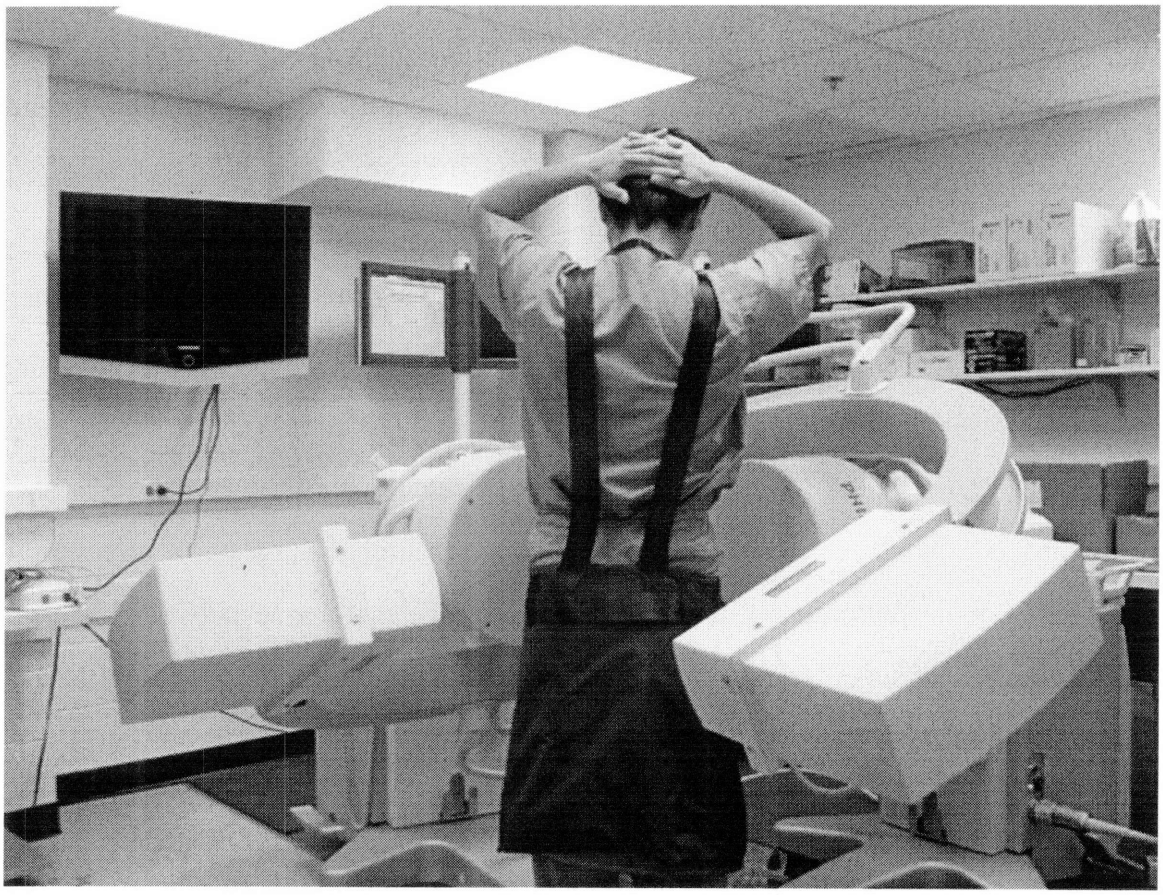

Figure 2-5: Two fluoroscopes positioned perpendicular to each other to capture the spine motion of subjects in the common view port.

The fluoroscopes use pulse snapshots to capture images. The fluoroscopes have a frame rate of 125Hz. 30, 15, or 8 snapshot images per second can be selected that are evenly distributed among the 125 Hz frame rate, which can efficiently reduce the radiation exposure under a high frame rate. The fluoroscope has a clearance of approximately 1 m between the X-ray source and the receiver, allowing the subject to be imaged by the fluoroscopes in real time as he or she actively performs different maneuvers. With a 1K x 1K resolution of both fluoroscopes, the total imaging volume can reach up to $30 \times 30 \times 30$ cm^3.

The fluoroscopic images suffer from small amounts of distortion caused by the slightly curved surface of the image intensifier and environmental perturbations of the x-ray. In order to remove "swirl" caused by electro-magnetic disturbance and "fish-eye" from the curved image surface a known grid is imaged and the subsequent image is mapped to the known geometry. A global surface mapping using a polynomial fitting technique adapted from Gronenschild is used to accomplish this [115]. A plexi-glass plate with a pattern of holes in concentric circles is used (**Fig 2-6**).

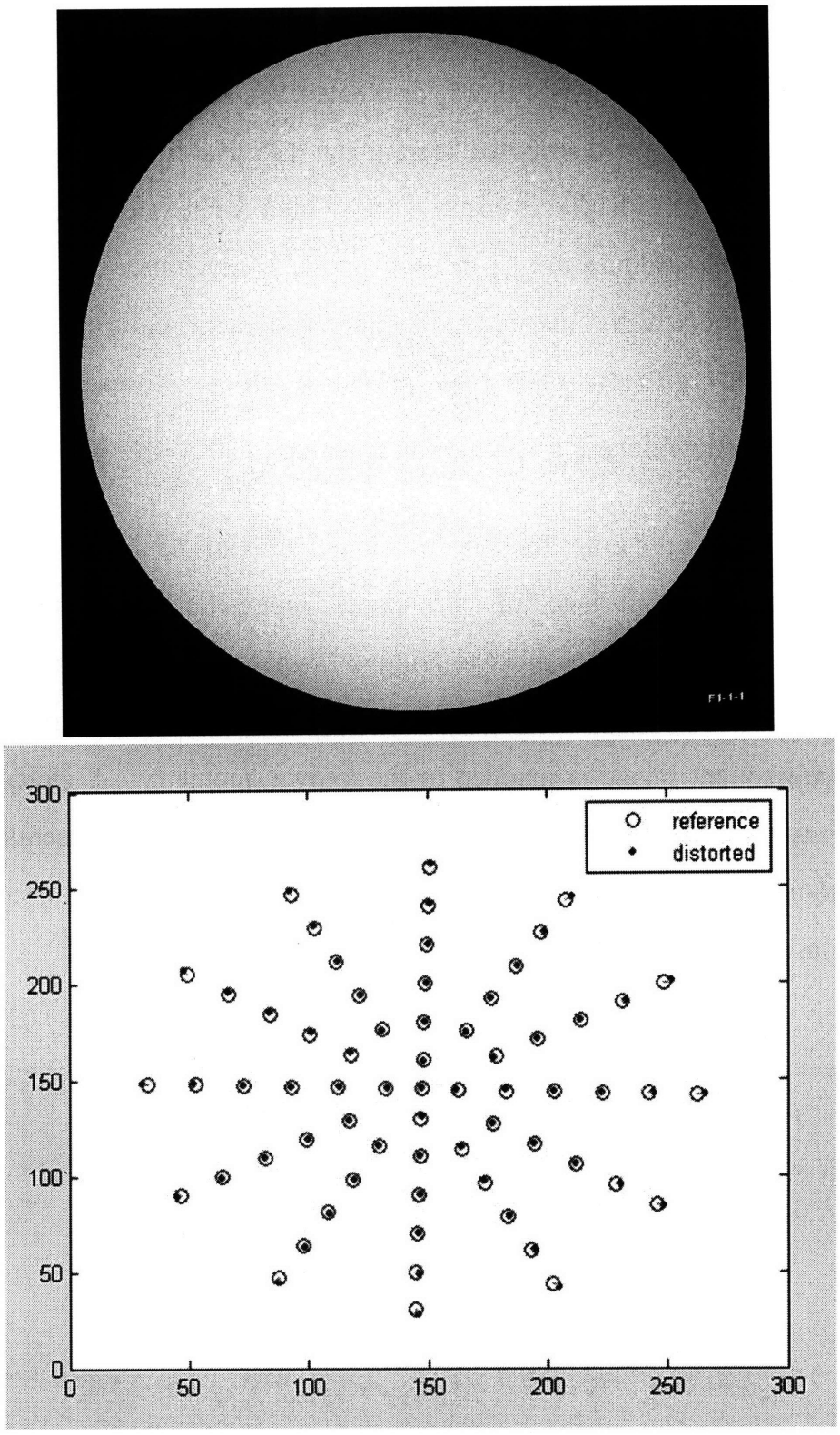

Figure 2-6: A patterned plexi-plate used to restore the distortion caused by fluoroscope to calibrate the captured spine image.

2.2 Matching

The geometry of the dual fluoroscopes from these tests was reproduced virtually in Rhinoceros. Pairs of fluoroscopic images were placed at the two virtual intensifiers. The CT/MR models of the vertebrae were introduced into the virtual system and viewed from the perspective views of the virtual sources. The 3D models were then independently translated and rotated in 6DOF until their outlines matched the osseous outlines of the fluoroscopic images from the two orthogonal views (**Fig. 2-7**).

The in-vivo positions of the vertebrae at various physiologic functional weightbearing positions can be reproduced in the Rhinoceros using the 3D models of the vertebrae and the orthogonal fluoroscopic images [12]. The pair of fluoroscopic images of the spine captured at a specific posture were imported into the modeling software and placed in calibrated orthogonal planes, reproducing the actual positions of the image intensifiers of the fluoroscopes. Two virtual cameras were created inside the virtual space to reproduce the positions of the x-ray sources with respect to the image intensifiers. Therefore, the geometry of the DFIS can be recreated in the solid modeling program. The MR or CT image-based 3D vertebral models will be introduced into the virtual fluoroscopic system and viewed from the perspective views of the two virtual cameras (**Fig. 2-7a**). The 3D models of the vertebrae could be independently translated and rotated in 6DOF until their outlines match the osseous outlines captured on the two orthogonal fluoroscopic images. This process can be executed using an existing protocol established in our laboratory [6]. The software allowed the model to be manually translated and rotated in increments of 0.01 mm and 0.01. Using this technique, the vertebral positions during in-vivo weightbearing activities are reproduced, representing the 6DOF kinematics at each in-vivo posture (**Fig. 7b**).

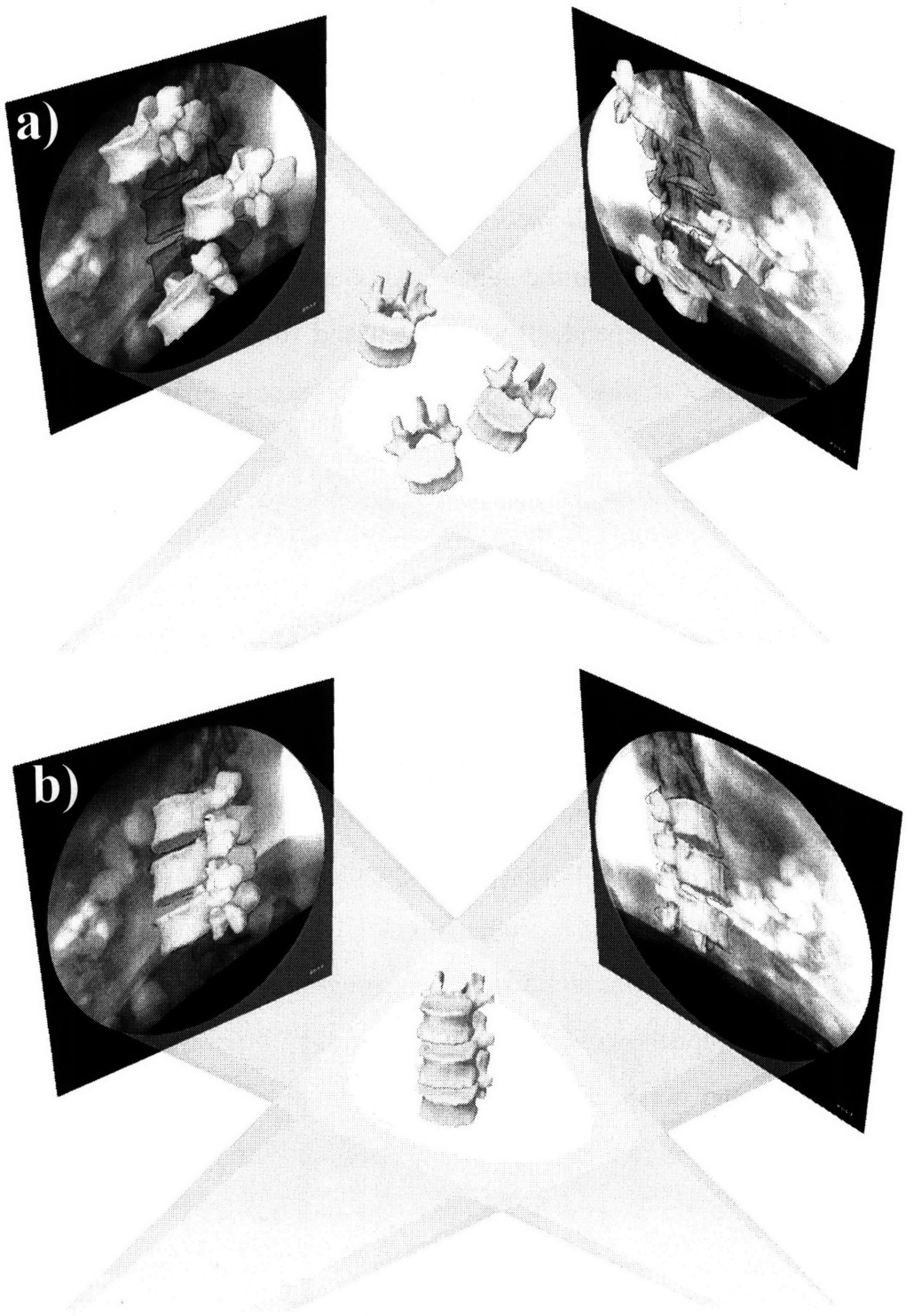

Figure 2-7 a) The 3D model of the lumbar spine segments (from human MRI) were introduced into virtual system reproduced from geometry of DFIS. b) After manipulate the model in 6DOF, kinematics of the spine can be studied from various physiologic functional activities.

After reproducing the in-vivo vertebral positions using the 3D anatomic vertebral models, the relative motions of the vertebrae can be analyzed using right hand Cartesian coordinate systems constructed at the center of each vertebra (**Fig. 2-8**). The geometric center of the vertebra body is chosen as the origin of the coordinate system. The x-axis is in frontal plane and pointed to the left direction; the y-axis is in sagittal plane and pointed to the posterior direction; and the z-axis was vertical to the x-y plane and pointed proximally.

The relative motions of the proximal vertebra with respect to the distal vertebra can be calculated at different vertebral levels. Three translations using x, y and z are defined as the motions of the proximal vertebral coordinate system origin in the distal coordinate system: anterior-posterior, left-right and distal-proximal translations. Three rotations using α, β and γ are defined as the orientations of the proximal vertebral coordinate system in the distal vertebral coordinate system using Euler angles (in x-y-z sequence): flexion-extension, left-right bending and left-right twisting rotations (**Fig. 2-8**).

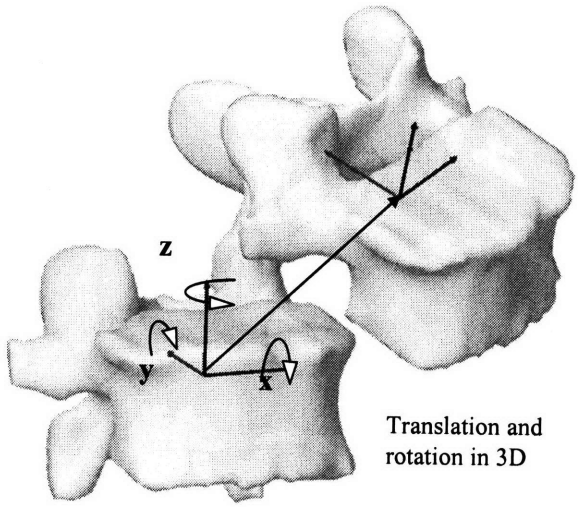

Figure 2-8: Coordinate system to describe 6DOF spine kinematics, both translational and rotational.

2.3 Summary

While many approaches to study spine kinematics and IVD deformation have been utilized, the quantitative understanding in the human spine under in-vivo physiologic functional activities is elusive. This study will utilize a newly developed, non-invasive imaging technique to quantitatively investigate the intrinsic biomechanics of human spine under physiologic functional activities. The subject underwent an MRI or CT scan to construct the 3D model of lumbar spine. The subject was then imaged by two fluoroscopes in two perpendicular views simultaneously at physiologic loading motions. MRI models were introduced into the virtual computer system and were independently translated and rotated in 6DOF until their projection matched the bony outlines of the two fluoroscopic images. The accuracy of this technique will be validated in the following Chapter. The technique will be applied on studying normal human subjects to obtain quantitative data to evaluate in-vivo vertebral motion in the later Chapter. The data will enhance our understanding of spinal pathology and to improve the current surgical treatment methods for spinal diseases that aim at restoring normal spine biomechanics.

Chapter 3

Validation

Limitations of current technology and the complex anatomy of the spine have made in-vivo data limited regarding the motion of the vertebrae under physiologic functional activities. To understand the biomechanical factors that affect spinal pathology, it is critical to accurately determine the spinal structural functions under in-vivo physiologic functional activities. In the previous chapter the idea for employee non-invasive image matching method has been illustrated. The accuracy and repeatability, however requires carefully validation before this method be efficiently applied in spine biomechanics study.

The validation of this technique was conducted in two phases. The in-vitro portion used an ovine spine specimen to validate the accuracy and repeatability of the combined imaging method when used to determine the spine positions in space. Both CT and MR based image models were constructed for the ovine vertebrae in this validation. The second phase was the application of this method to a living human subject in order to determine if the repeatability of the method was maintained under in-vivo conditions. Only MR model has been utilized to minimize the radiation dosage to the subject. The goal is to investigate the feasibility for clinical application of the novel technique.

3.1 In-vitro validation

3.1.1 CT and MR models

An ovine lumbar spine specimen, [116] with all the surrounding soft tissues intact was selected and L2 and L3 vertebrae were focused for this study. The spine was CT and then MR scanned according to the protocol in Chapter 2. The contours of L2 and L3 were digitized from both CT and MR images to reconstruct 3D mesh models. The constructed CT and MR image-based models were then mapped together using a customized code implemented in the Matlab based on the ICP method. A local coordinate system was created for each spine vertebral segment model. For the purpose of comparison, the same coordinate system was used by both models. In this study, 6DOF was expressed using the x, y and z axes for left/right, anterior/posterior and up/down translations and using α, β and γ for the Euler angel flexion/extension, left/right bending and internal/external rotation of the vertebrae (**Fig 3-1**).

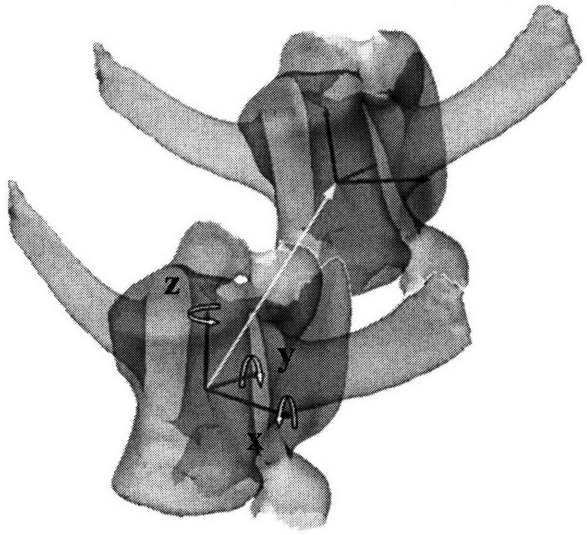

Figure 3-1: A demonstration of local coordinate system established to determine 6DOF kinematics of the ovine lumbar spine.

3.1.2 *Dual fluoroscopes section*

The DFIS consists of two fluoroscopes positioned perpendicular to each other to capture images of the spine segments simultaneously (detailed in Chapter 2). The specimen was imaged during two tests using DFIS to validate the accuracy and repeatability. First, a gold standard for precisely obtain spine positions was chosen by using an MTS material test machine (MTS Qtest 5, Minneapolis, MN). The MTS machine has an accuracy of 0.001 mm in translation. The specimen was bounded to the MTS machine which moves vertically upward at 1000 mm/min while dynamic images were taken by the DFIS. (**Fig. 3-2**)

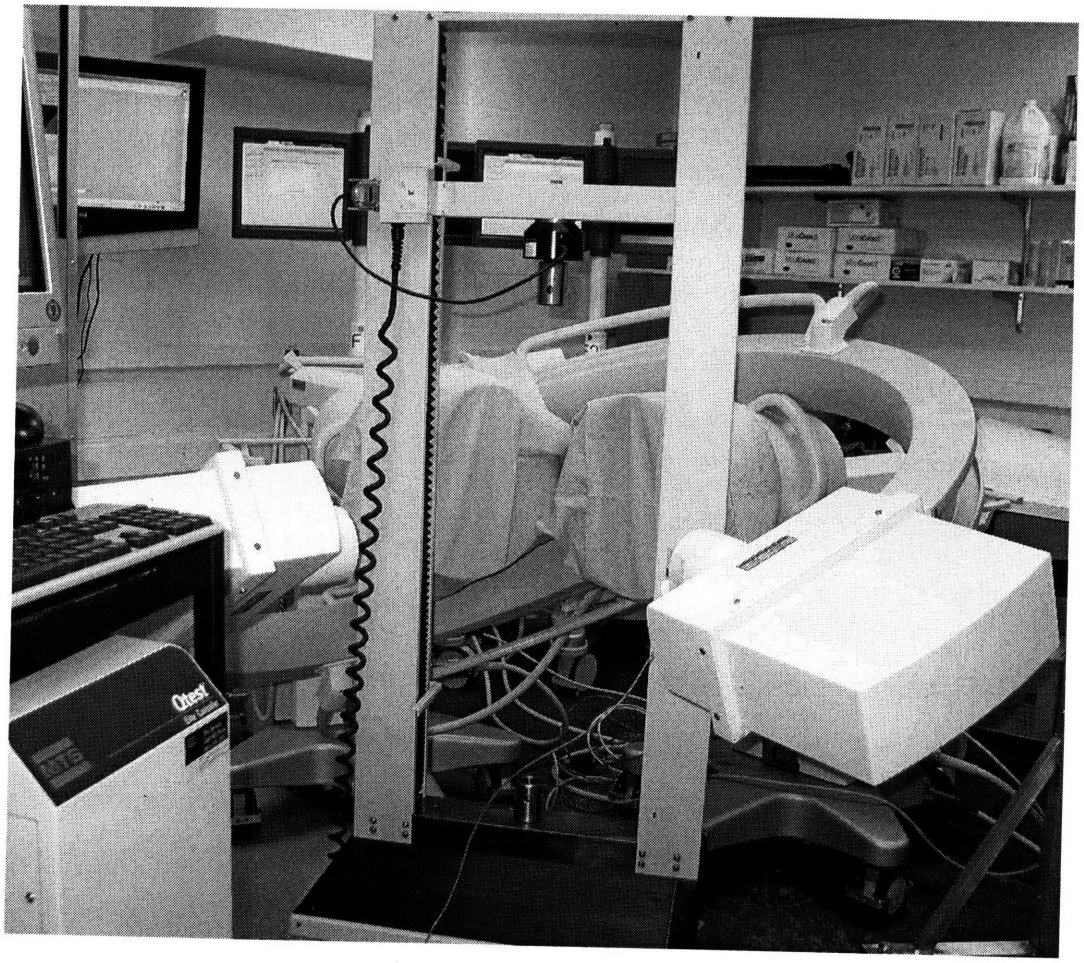

Figure 3-2: The MTS material test machine was setup to move spine specimen in the common field of view of DFIS to perform a validation test on the accuracy.

This test was aimed to validate the accuracy of the image system in determination of spine translation and speed. In the other test, the specimen was manually flexed to simulate dynamic physiologic flexion-extension motion (**Fig. 3-3**). Dynamic orthogonal images were taken simultaneously from the posteromedial and posterolateral directions aimed at the target spinal segment.

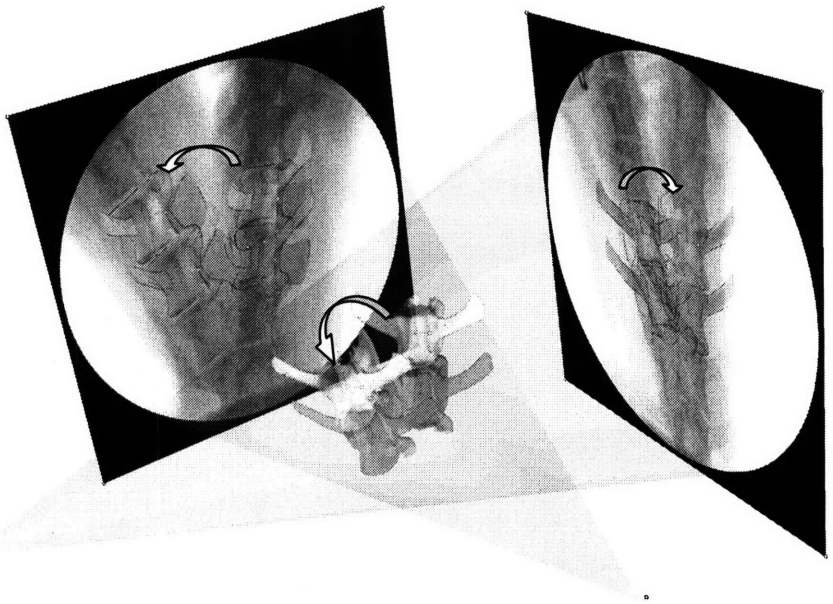

Figure 3-3: The specimen was manually flexed to simulate a physiologic motion when two fluoroscopes captured images simultaneously. The test was designed to validate the repeatability of matching spine motion.

The spatial positions of the vertebral bodies during the motion on the MTS machine and the manual flexion-extension activities were reproduced in Rhinoceros software, using the 3D models of the spinal segments combined with the orthogonal fluoroscopic images. First, the geometry of the two fluoroscopes from the two tests was reproduced virtually in Rhinoceros software. Pairs of fluoroscopic images captured at a specific time were placed at the two virtual intensifiers. The CT/MR models of the vertebrae were introduced into the virtual

system and viewed from the perspective views of the virtual sources. The 3D models were then independently translated and rotated in 6DOF until their outlines matched the osseous outlines of the fluoroscopic images from the two orthogonal views (**Fig. 3-4**). Using this technique, the vertebral positions during various spine activities could be reproduced and represented using the 6DOF positions of the 3D vertebral models in space.

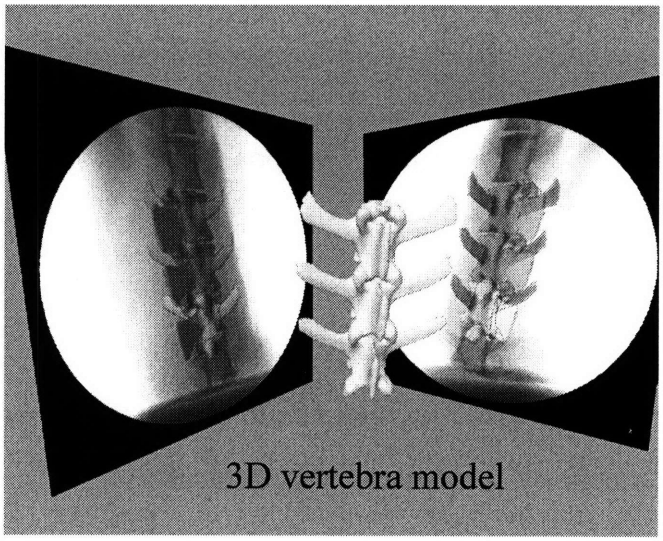

Figure 3-4: After matching the 3D model with 2D orthogonal fluoroscopic images sets from DFIS, the kinematics of the spine was reproduced in space.

3.1.3 Accuracy and repeatability analysis

To evaluate the accuracy of the image matching technique in reproducing vertebral motion, three positions were chosen from the dynamic motion path of the spine that was created using the MTS machine. The exact (to four decimal places) time for each position was obtained from the fluoroscopic radiation impulse data file recorded during the experiment. The distances moved by the MTS machine between the 3 positions were calculated from these time intervals and the known MTS speed. Each of the 3 positions was reproduced 5 times independently using both the CT and MR models and the dual fluoroscopic images as illustrated in the

inset figure in **Table 3-1**. The displacements of the L2 and L3 vertebrae were calculated between the 3 positions. The translational speed of the vertebra was calculated between the different positions. The displacement and speed data obtained from the 5 model image matching processes were averaged and expressed as mean ± standard deviation (SD). These data were compared with those of the MTS machine (gold standard) to examine the accuracy of the image model matching method in reproducing the spine translation and speed.

To evaluate the repeatability of using the image matching method to reproduce the dynamic spine motion, five positions along the manual dynamic flexion-extension path were determined 5 times using both the CT and MRI based models and the corresponding dual fluoroscopic images. The positions and orientations of the L3 with respect to L2 vertebrae were calculated at each selected flexion-extension position. SD of the 6DOF kinematics reproduced by the 5 image modeling matching processes were calculated. The repeatability in reproducing the relative positions of the L3 and L2 using the image model matching method was calculated using the average SD of the 5 positions of the spine along the flexion-extension path.

			P 2-1	P 3-2	P 3-1
Distance (mm)	MTS		33.32 mm	33.33 mm	66.64 mm
	CT	L2	33.52 ± 0.18	33.27 ± 0.09	66.81 ± 0.19
		L3	33.39 ± 0.17	33.15 ± 0.13	66.55 ± 0.14
	MRI	L2	33.72 ± 0.35	33.14 ± 0.32	66.88 ± 0.23
		L3	33.23 ± 0.25	33.35 ± 0.17	66.72 ± 0.19
Speed (mm/s)	MTS		16.67 (mm/s)		
	CT	L2	16.77 ± 0.09	16.64 ± 0.04	16.71 ± 0.05
		L3	16.71 ± 0.09	16.56 ± 0.07	16.64 ± 0.03
	MRI	L2	16.87 ± 0.17	16.56 ± 0.16	16.72 ± 0.06
		L3	16.63 ± 0.13	16.66 ± 0.08	16.65 ± 0.05

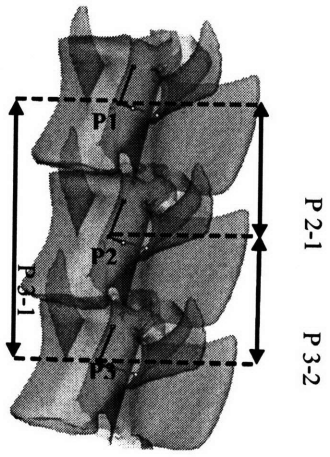

Table 3-1: Accuracy test of the DFIS obtained from comparing vertebrae motion distance and speed prescribed by the MTS machine with the reproduced kinematics.

The displacements of the spine segment between the three positions along the MTS moving path were 33.32 mm (P1-P2), 33.33 mm (P2-P3) and 66.64 mm (P1-P3), respectively, for both L2 and L3 vertebra. The model matching process showed a high accuracy in determining the positions of the spinal segments (**Table 3-1**). Both CT and MR image-based models could determine the spine traveling distances with an absolute mean accuracy below 0.2 mm. The maximal differences compared to those of the MTS machine measurements were 0.20 mm for the CT model and 0.40 mm for the MR model. Compared with the standard MTS speed of 16.67 mm/s, the CT model reproduced a speed between 16.58 and 16.77 mm/s. The MR model reproduced a speed between 16.57 and 16.87 mm/s. The absolute speed errors were within 0.2 mm/s for both CT and MR models. The accuracy validation using the MTS as a gold standard did not show a significant difference between CT and MR model matching ($p=0.2$) in determination of traveling distance and speed of the spine.

To evaluate the repeatability, we determined the SD of the 5 matching trials for five positions along the flexion-extension path of the spine segment. The matching process of the dual orthogonal fluoroscopic system was found to be highly repeatable in determining the 6DOF positions and orientations of the vertebrae using both the CT and MR models (**Table 3-2**). The relative position and orientation of L2 with respect to L3 were determined with a SD less than 0.2 mm using the CT model and 0.25 mm using the MR model. The relative orientation could be determined to be 0.4° to 0.6° for CT model and 0.6° to 0.9° for MR model.

	x	y	z	α	β	γ
CT L3-L2	0.18	0.11	0.18	0.42	0.59	0.53
MR L3-L2	0.26	0.18	0.25	0.55	0.79	0.89

Table 3-2: Repeatability of reproducing the relative positions of the L3 with respect to L2. The data were averages of standard deviations at 5 positions along the flexion-extension motion path.

3.1.4 Conclusion and discussion

We have developed an imaging matching technique using 3D anatomic vertebral models and DFIS to measure in-vivo spine kinematics. The models were obtained from both CT and MR. Two tests were designed using DFIS to evaluate accuracy and repeatability of this technique. In literature, a few pioneer studies have investigated spinal vertebral motion using CT imaging [16,23,72-74,79] with accuracy larger than 1 mm in translation and 1° in orientation. The MR combined DFIS technique is able to determine an absolute mean accuracy within 0.2 mm in translations and a repeatability within 0.3 mm and 0.9° in translations and rotations.

The MR models resulted in similar and sufficient accuracy and repeatability for the purpose of this study compare to CT models either from our study or from the literature. CT images may facilitate automatic segmentation with commercially available software. In contrast, automatic segmentation for MR models is currently time consuming. However, the dosage of radiation to which the subjects are exposed when utilizing CT imaging may present an ethical concern for the safety of the individuals being tested. Alternatively, MR model provide us with greater visualization of the ligamentous components surrounding the lumbar vertebra as well as their relation to relevant neurologic structures in this area. Therefore, in order to minimize the risk to the application on living

human subjects involved in Chapter 4 and to enhance our ability to look at the soft-tissue structures of the lumbar spine for further study on pathology, we will use MR imaging exclusively.

3.2 In-vivo validation

Consider the potential anatomic and functional difference between the ovine and human, a validation test was designed to evaluate the repeatability of the model matching method in the determination of in-vivo vertebral kinematics. The image matching method was applied to a living subject (Female, 60 years old). Prior to the initiation of the study, approval by the institutional review board (IRB) was obtained. The subject signed the consent form and was evaluated for the absence of LBP and other spinal disorders.

3.2.1 MR models

The subject underwent an MR scan of the lumbar spine using a surface coil and a T2 weighted fat suppressed 3D SPGR sequence, the same protocol as in Chapter 2 and used for the ovine spine. The 3D MR images were used to construct the 3D model of lumbar spine. A CT scan was not performed to avoid the cumulative radiation dosage on the subject.

3.2.2 Dual fluoroscopes section

The subject was first asked to stand in the dual fluoroscopic image system (**Fig. 3-5a**) to image the lumbar spine position in the standing weight-bearing posture. The subject was protected by specifically designed lead vests and skirts. The subject was then imaged in the following sequence of positions: maximal left twist, maximal right twist, and forward flexion at approximately 45°. Using the matching method, the relative position of the L2 with respect to L3 vertebra was

reproduced 5 times (**Fig. 3-5b**). In this study, 6DOF was expressed using the vertebral displacements along the x, y and z axes for medial/lateral, anterior/posterior and up/down translations and using α, β and γ for the flexion/extension, medial/lateral bending and internal/external rotations of the vertebrae (**Fig. 3-6**). The repeatability of this technique to evaluate in-vivo kinematics of the human lumbar spine was represented by the SD of 6DOF translations and rotations from the 5 matchings at each in-vivo position of the spine.

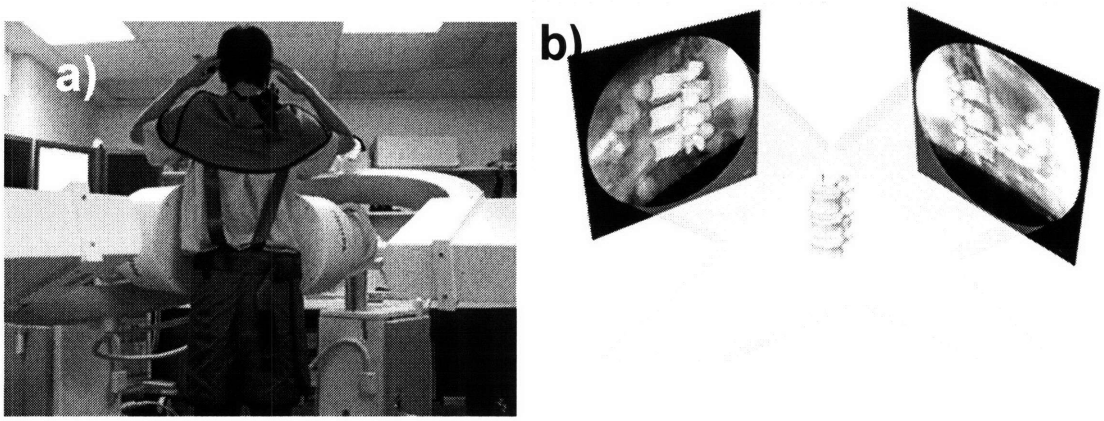

Figure 3-5: a) Dual Fluoroscopic setup for imaging of the lumbar spine position in living subjects during various physiologic functional activities. b) The virtual dual fluoroscopic system is established in Rhinoceros to reproduce in-vivo spine positing using the fluoroscopic images and the 3D vertebral models.

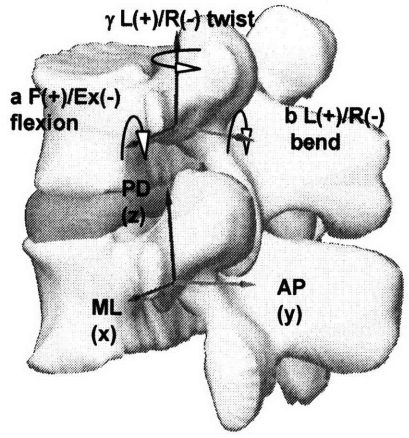

Figure 3-6: 3D vertebral models and local coordinate systems that were used to determine 6DOF kinematics.

3.2.3 Results and discussion

The repeatability in reproducing in-vivo human spine kinematics (the relative positions of the L2 segment with respect to the L3 segment) was shown in **Table 3-3** for various in-vivo spine positions. For all the in-vivo physiologic loading positions, the relative translation could be determined within a SD of 0.3 mm, while the orientation could be determined within 0.7°, which is comparable with the ovine validation studies from 3.1. The relative position of L2 with respect to L3 was also reproduced using the MR combined DFIS matching method. For example, in forward flexion, the position of L3 with respect to L2 was determined to be -0.79 ± 0.30, 2.23 ± 0.22 and -36.75 ± 0.22 mm in medial, posterior and distal directions and 3.52 ± 0.56°, 3.81 ± 0.62° and 4.30 ± 0.63° in forward flexion, left bending and left axial twist. However, these data will be saved and further studied and discussed for the application on human lumbar spine kinematics in Chapter 4.

	X L(+)/R(-) trans	Y A(-)/P(+) trans	Z U(+)/D(-) trans	α Fl(+)/Ex(-) flex	β L(+)/R(-) bend	γ L(+)/R(-) twist
MRI Position	-0.21	1.2	-36.78	10.29	2.42	1.54
Standing	-1.16 ± 0.29	2.86 ± 0.28	-35.71 ± 0.21	7.80 ± 0.46	4.03 ± 0.65	7.02 ± 0.47
Flexion	-0.79 ± 0.30	2.23 ± 0.22	-36.75 ± 0.22	3.52 ± 0.56	3.81 ± 0.62	4.30 ± 0.63
Twist left	-1.52 ± 0.29	3.00 ± 0.27	-35.53 ± 0.23	10.89 ± 0.68	7.13 ± 0.56	7.20 ± 0.43
Twist right	1.13 ± 0.33	3.19 ± 0.24	-35.35 ± 0.18	12.87 ± 0.75	-0.41 ± 0.66	9.98 ± 0.56

Table 3-3: Repeatability of reproducing the relative positions of L3 with respect to L2 using the DFIS when the living subject moved to different positions. The repeatability was represented by mean ± standard deviation of the 5 model matchings.

3.3 Summary

Quantitative knowledge of in-vivo vertebral kinematics is instrumental in understanding spinal pathology and for the improvement of the surgical treatment of spinal degenerative disease. The MR combined DFIS image matching method showed a potential way for non-invasive study in-vivo spine biomechanics under physiologic functional weightbearing activities. This Chapter presented a rigorous validation of the MR (and CT) combined DFIS image matching technique for the non-invasive measurement of spinal motion. The accuracy of this technique was first validated for the determination of vertebral position using an in-vitro experimental setup since a gold standard for vertebral positions was able to be established from MTS machine. The data indicated that the method has accuracy within 0.2 mm in determination of vertebra translations and 0.2 mm/s in translational speed. The repeatability of the method was then examined using both in-vitro and in-vivo experimental design setups. Both the CT and MR image-based model showed similar accuracy and repeatability in the in-vitro tests. The in-vivo human spine experiment using MR model demonstrated a high

repeatability of the method in determination of vertebra within 0.3 mm and 0.6° for translation and orientation.

It should be pointed out that, despite the highly accurate and reliable results obtained during the validation trial, there has certainly been a considerable learning curve during the process of developing this technique. This applies not only to our ability to perform this technique but also to obtain images that are most suitable for the study. It is also significantly more difficult to image in-vivo subjects as motion artifact becomes a concern. We anticipate that there will be a progressive improvement in our ability to obtain fluoroscopic and MR images that were not available at the time of this study. The MR sequences are continuously undergoing adjustment during our ongoing studies in order to improve the resolution of the anatomic features. We therefore anticipate that with further refinement of our technique, coupled with technological advancements in fluoroscopic and MR imaging modalities, the accuracy and reliability of our technique will be improved.

In conclusion, this Chapter examined the accuracy and repeatability of a novel imaging technique in the determination of 6DOF kinematics of lumbar spine segments in a non-invasive manner. The in-vitro validation indicated that this method is accurate in determination of vertebral position in space. Therefore, the MR combined DFIS imaging technique can be a useful tool to investigate in-vivo spine biomechanics, such as to determine vertebral positions and orientations before and after surgical procedures for the treatment of diseased spinal segments in order to evaluate the efficacy of these various surgical modalities in restoring normal spine function. An example of potential applications of this technique includes the evaluation of the effects of spinal fusion or total disc replacement and their effects on adjacent unaffected segments. In the following Chapter, the

method will be applied for the investigation of vertebral motion of living human subjects under various in-vivo physiologic conditions.

Chapter 4

Application on Spine Biomechanics Study

Accurate knowledge of the physiological kinematics of the lumbar spine vertebrae is important to the understanding of the etiology of spinal diseases such as discogenic lower back pain. This knowledge is also necessary for the improvement of surgical treatments of spinal diseases that involve either segmental arthrodesis (fusion) or artificial disc arthroplasty (replacement) which may alter the vertebral motion patterns. In-vitro experiments using cadaveric spinal segments have been pursued for decades in order to understand spinal biomechanics [27,117,118]. Numerous studies have reported on spine kinematics [15-26] and corresponding deformation [37-43,45-52,119] when a spine segment specimen was subjected to simulated functional activities.

In order to better understand the biomechanical factors that affect spinal pathology among treated patients, it is necessary to determine the spinal kinematics in living human subjects. However, the limitations of current technology and the complex anatomy of the lumbar spine have made it difficult to measure the vertebral motion under physiologic functional activities. In-vivo spinal research to date has mainly concentrated on the measurement of range of motion (ROM) and the evaluation for instability using methods such as bilateral radiographs, MRI [81,83,84,87,88], CT [73], electrogoniometer [102-105], and videofluoroscopy [28,120]. For example, early research used plain radiographs to examine the spinal motion of living subjects during flexion-extension positions [121,122]. Subsequently, MR imaging technique [123-125] and CT-based methodology [79,126] have been used to measure 3D spinal segmental positions in human subjects

while lying in supine positions.

In the previous Chapter, the MR combined DFIS imaging method has been validated on spine kinematics study. The system was shown to be appropriate for the investigation of lumbar spine motion during weightbearing functional activities. In this Chapter, this technique was first used to determine the 6DOF vertebral motion of the lumbar spine of living human subjects in various weightbearing positions of the body. Then based on the 6DOF kinematics data from these positions, disc deformation was quantitatively studied.

4.1 Experiment setup

Eleven asymptomatic subjects with age ranging from 50-60 years (5 males and 6 females) were recruited for this study. Approval of the institutional review board (IRB) was obtained prior to the initiation of the study. The subjects were evaluated for the absence of lower back pain and other spinal disorders. A signed consent form was obtained from each subject before any testing was performed.

First, the lumbar segments of each subject were MR scanned with a spine surface coil and a T2 weighted fat suppressed 3D SPGR sequence (same as in Chapter 2 and 3). The subject warmed up for about 30 minutes and then scanned in a supine, relaxed position. The MR images of each subject were carefully examined. Two subjects were found to have presence of early disc degeneration in the absence of clinical symptoms. Additionally, one subject was found to have early scoliosis without symptoms. These three subjects were excluded from further investigation. The MR images of the lumbar spinal segments were then imported into a solid modeling software Rhinoceros to construct 3D anatomical

vertebral models of L2, L3, L4 and L5 of the lumbar spine using the same protocol in Chapter 2 and 3. (**Fig. 4-1**)

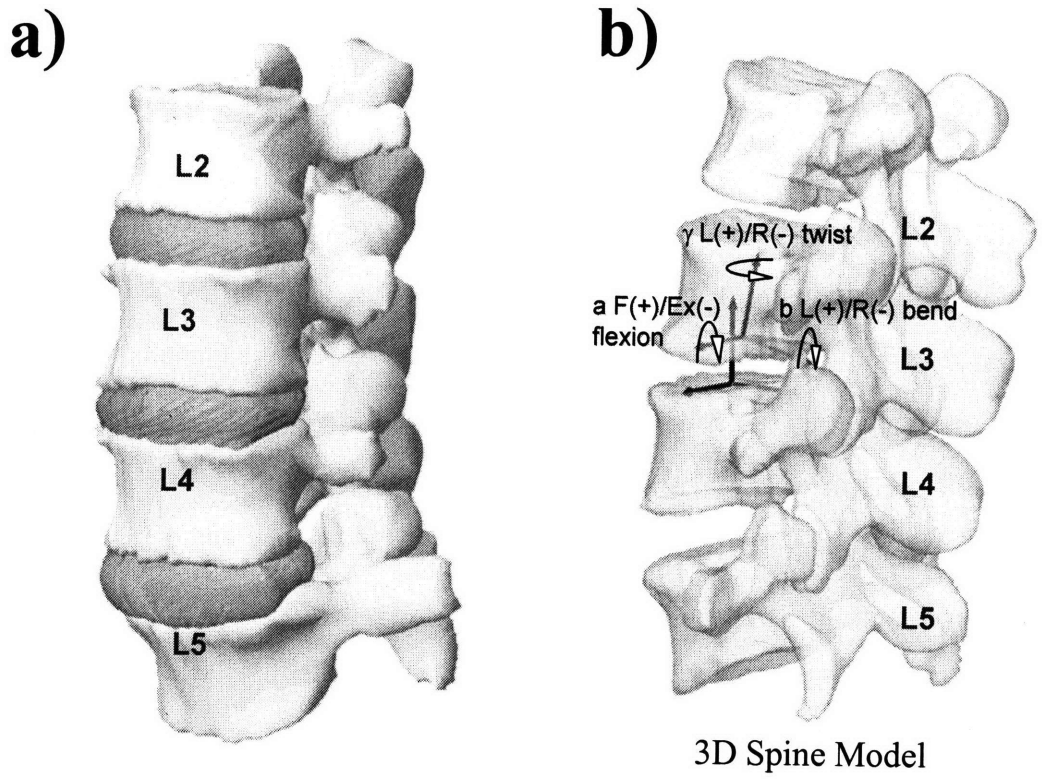

Figure 4-1: a) 3D lumbar spine model was constructed from MRI scans. b) The local coordinate systems were established at the center of endplate to study the relative motion of two adjacent vertebral bodies.

Following MR scanning, the lumbar spines of the subjects were imaged using the DFIS. During fluoroscopic imaging, the subject was protected from radiation exposure with appropriate lead shielding. The subject was protected from above and below their lumbar spine by specifically designed skirts, vests, and thyroid shields. A surgeon constantly checked the lead protections to ensure that they did not slip away during the experiment.

The target spinal segments were then exposed to fluoroscopic scanning. The subject was asked to stand and positioned their lumbar spines within the view of both fluoroscopes and actively moved to different postures in a predetermined sequence: standing position; 45° flexion; maximal extension; maximal left-right bending; maximal left-right twisting. The two laser pointers attached to the fluoroscopes helped to position the target lumbar spine segments inside the field of view of the two fluoroscopes. At each selected posture, two orthogonal images were taken simultaneously from two directions of the targeted spinal segment. The subject then moved to the next posture under the direction of an orthopaedic surgeon. Care was taken to ensure that no constraint was applied to the hips of the subjects while performing the active motions. During testing, the subject was exposed to approximately 10 pairs of fluoroscopic projections. The entire experiment took about 10 minutes. The images were processed in the Digital Imaging and Communications in Medicine (DICOM) and Bitmap file formats.

The in-vivo positions of the vertebrae at various weightbearing body positions were reproduced in the Rhinoceros the 3D models of the vertebrae and the orthogonal fluoroscopic images. First, the geometry of the dual-orthogonal fluoroscopic system was recreated in Rhinoceros. The MR image-based 3D vertebral models were then introduced into the virtual fluoroscopic system to be independently translated and rotated in 6DOF until their outlines match the osseous outlines captured on both fluoroscopic images. This process was discussed in details in Chapter 2. Using this technique, the vertebral positions during in-vivo weightbearing activities were reproduced, representing the 6DOF kinematics of the vertebrae at each in-vivo posture (**Fig. 4-2**).

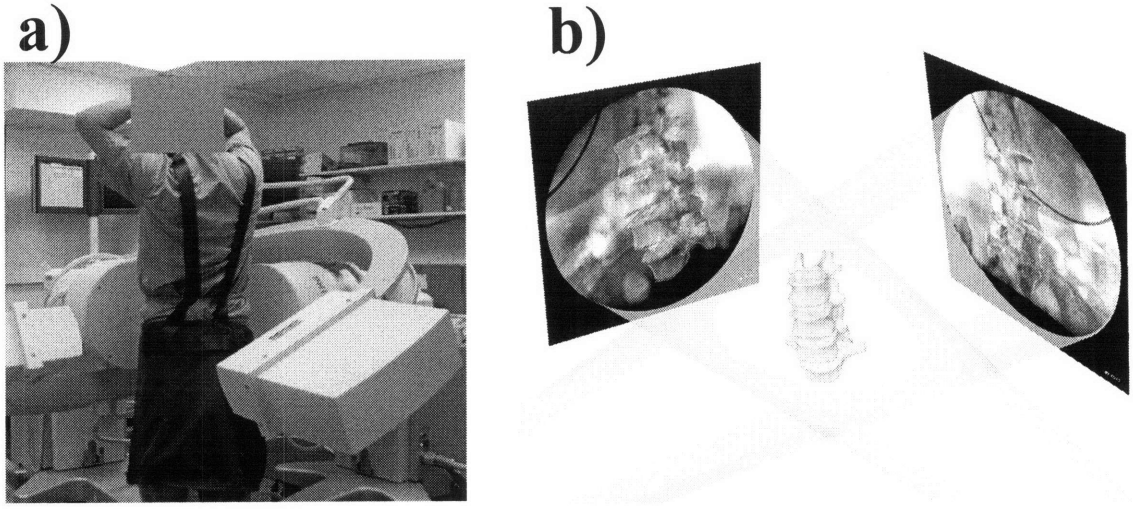

Figure 4-2: a) The experimental setup of the dual fluoroscopic system for capturing the lumbar spine positions of living subjects. b) The virtual DFIS that mimics the actual fluoroscopic system was used to reproduce the in-vivo vertebral positions.

4.1.1 Vertebrae range of motion

After reproducing the in-vivo vertebral positions using the 3D anatomic vertebral models, the relative motions of the vertebrae were analyzed using right hand Cartesian coordinate systems constructed at the endplates of each vertebra (**Fig. 4-1**). The geometric center of the endplate was chosen as the origin of the coordinate system. The x-axis was in frontal plane and pointed to the left direction; the y-axis was in sagittal plane and pointed to the posterior direction; and the z-axis was perpendicular to the x-y plane and pointed upward.

The relative motions of the proximal vertebrae with respect to the distal vertebrae were calculated at 3 vertebral levels: L2-3, L3-4 and L4-5. Three translations were defined as the motions of the proximal vertebral coordinate system origin in the distal coordinate system: anterior-posterior, left-right and distal-proximal translations. Three rotations were defined as the orientations of the proximal vertebral coordinate system in the distal vertebral coordinate system

using Euler angles (in x-y-z sequence): flexion-extension, left-right bending and left-right twisting rotations (**Fig. 4-1b**).

After the determination of vertebral positions at each posture, we determined the ROM of each vertebral level between flexion-extension, left-right bending and left-right twisting. The ROM data included both the primary rotations and coupled translations and rotations in the other 5 degrees of freedom. A repeated measure ANOVA was used to compare the ROM at L2-3, L3-4 and L4-5 vertebral levels at each of the 3 functional activities. Statistic significance was set when $p < 0.05$.

4.1.2 In-vivo disc deformation

Quantify in-vivo disc deformation is a critical but missing area in spine research to under various clinic problems, such as to delineate the mechanisms of post-operative adjacent DDD, and to improve our current surgical modalities. Due to the non-invasive manner to the new DFIS combined MRI technique, deformation of the disc during physiologic functional activities were studied. The disc shapes in 3D were quantitatively determined using the two adjacent vertebral kinematics (L23, L34 and L45), more specifically, using the relative positions and orientations of the endplates. Five pairs of mark points, which locate at anterior/posterior, left/right edges and center of the disc, were picked from the disc. The distance between mark points during standing, twisting, bending and flexion were compared to MRI position to determine the disc deformation.

The disc shape obtained in the standing position will be used as a reference since the spine is under a non weight-bearing condition. The distance between each pair of mark points on the two disc attachments (**Fig. 4-3**) will be compared before (l_0) and after (l_a) motion in the software. The geometric deformation is

defined as the distance change between pairs of points normalized by the distance measured from standing position of the disc, i.e, in the formula $(l_a - l_0)/l_0$. This will give out the geometric deformation distribution in different locations of the disc. Positive values represent tensile deformation and negative values indicate compressive deformation.

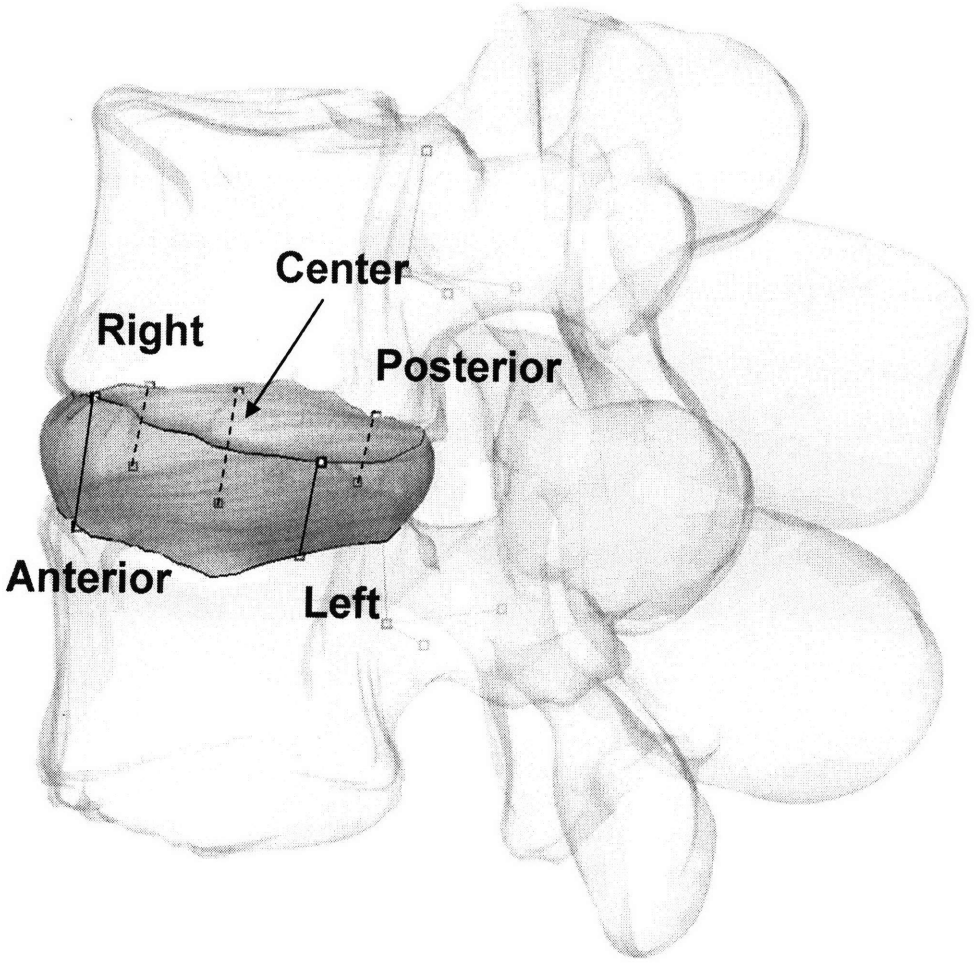

$$\text{Geometric Deformation} = \frac{\text{deformed length} - \text{original length original length (MRI)}}{}$$

Figure 4-3: A 3D view of the intervertebral disc of the in-vivo position of the lumbar spine. The change in length of the different potions of the disc can quantify disc deformation.

4.2 Results

4.2.1 Vertebrae range of motion

Primary rotations

The vertebrae at different vertebral levels had different range of flexion during the designed flexion-extension motion (**Fig. 4-4a**). The flexion ranges were 5.4±3.8°, 4.3±3.4° and 1.9±1.1° for L2-3, L3-4 and L4-5 levels, respectively. The L2-3 and L3-4 measurements are not statistically different in flexion range. However, both levels had significantly higher flexion ranges than the L4-5 vertebral level ($p<0.05$).

During the left-right twist activity, the 3 vertebral levels showed no significant difference in the range of twist rotations (**Fig. 4-4b**). The twist rotation ranges were 2.5±2.3° for L2-3, 2.4±2.6° for L3-4 and 2.9±2.1° for L4-5.

During left-right bending motion, the upper level generally had less range of bending rotation than the lower level (**Fig. 4-4c**). The L2-3 and L3-4 had left-right bending rotation ranges of 2.9±2.4° and 3.4±2.1°, respectively, but not statistically different. The L4-5 had a range of rotation during bending of 4.7±2.4°, which was statistically larger than those at both L2-3 and L3-4 levels.

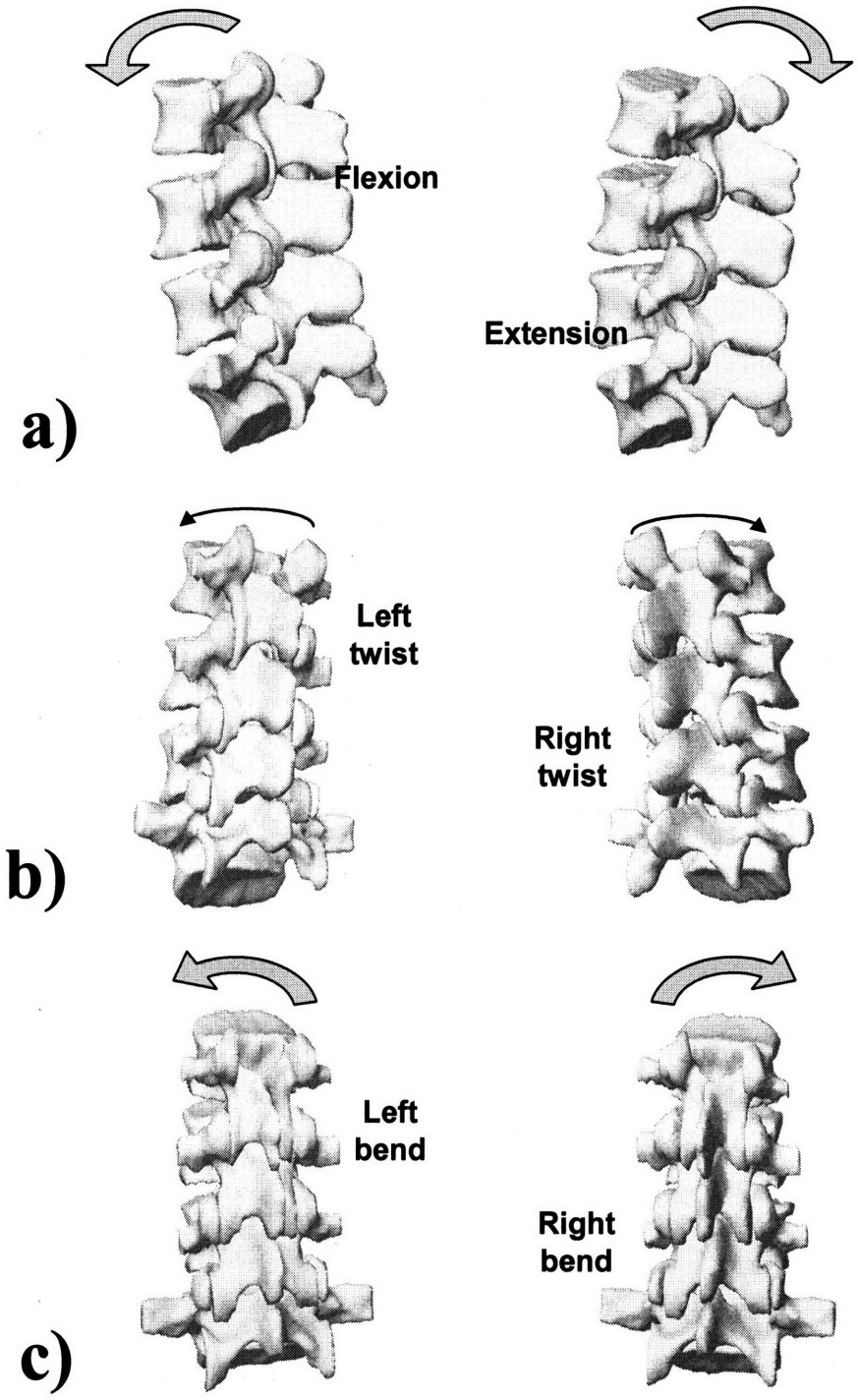

Figure 4-4: a) In-vivo lumbar spine in flexion and extension. b) In-vivo lumbar spine in left and right twist. c) In-vivo lumbar spine in left and right bending.

Coupled translations and rotations

During the active flexion-extension motion, there were coupled translations in all three directions (**Table 4-1**). On average, the translation range in left-right and anterior-posterior directions was between 0.7 and 1.5 mm. The coupled translation in proximal-distal direction is significantly lower at L2-3 (0.2±0.2 mm) than at L3-4 (0.6±0.4 mm) and L4-5 (0.7±0.6 mm). The coupled rotations in left-right bending and twisting were also similar and were, on average, between 1.7° and 2.9° (**Fig 4-5**).

During the active left-right bending motion, the coupled translations in left-right and anterior-posterior directions were similar in all the vertebral levels and on average, ranged between 0.8 and 1.1 mm (**Table 4-1**). The coupled translation in proximal-distal direction (between 0.4 and 0.6 mm) was lower compared to those at the other directions ($p<0.05$). The coupled flexion rotation range was between 1.3° and 2.1° at the L2-3, L3-4 and L4-5 levels, which was lower than their corresponding primary bending rotations ($p<0.05$). However, the coupled twist rotations were at similar magnitudes as the primary bending rotation; ranged between 2.2° and 3.8°.

During the active left-right twisting motion, on average, the translation in anterior-posterior direction was between 1.1 and 1.2 mm, while in left-right direction was between 0.5 and 1.0 mm. The coupled translation in proximal-distal direction was between 0.3 and 0.6 mm, which in general was lower than the coupled motion in the other two directions (**Table 4-1**). The coupled flexion range was between 0.9° and 2.3° which was lower in magnitude than the primary twist rotations. The coupled bending rotation was similar to the primary rotation, 2.0° and 3.0° (**Table 4-1**).

		Translation (mm)			Rotation (°)		
		LR	AP	PD	FE	Bend	Twist
		Flexion and extension					
L2_3	Mean	1.5	1.0	0.2	5.4	2.3	1.9
	SD	0.9	0.8	0.2	3.8	2.6	2.1
L3_4	Mean	1.1	0.7	0.6	4.3	2.0	1.7
	SD	0.7	0.6	0.4	3.4	1.6	1.5
L4_5	Mean	1.0	1.4	0.7	1.9	2.1	2.9
	SD	0.7	1.1	0.6	1.1	1.8	2.9
		Bending left and right					
L2_3	Mean	0.9	0.8	0.4	2.1	2.9	2.2
	SD	0.4	0.6	0.4	1.2	2.4	2.2
L3_4	Mean	0.8	0.8	0.3	1.3	3.4	3.8
	SD	0.9	0.7	0.2	0.8	2.1	2.3
L4_5	Mean	1.0	1.1	0.6	1.9	4.7	2.8
	SD	0.6	1.2	0.4	2.1	2.4	2.6
		Twisting left and right					
L2_3	Mean	0.7	1.1	0.6	1.7	2.6	2.5
	SD	0.4	0.7	0.5	2.9	1.2	2.3
L3_4	Mean	1.0	1.2	0.4	2.3	2.0	2.4
	SD	0.9	1.1	0.3	2.9	2.0	2.6
L4_5	Mean	0.5	1.1	0.3	0.9	3.0	2.9
	SD	0.6	0.6	0.2	0.8	1.6	2.1

Table 4-1: The range of motion of the lumbar spine at different levels during the various functional activities. During each activity, the highlighted primary rotations as well as coupled translation and rotations are presented to quantify 6DOF kinematics, including 3 translations LR (left-right translation), AP (anterior-posterior translation) and PD (proximal-distal translation); and 3 rotations FE (flexion extension), Bend (left-right bending) and Twist (left-right twisting).

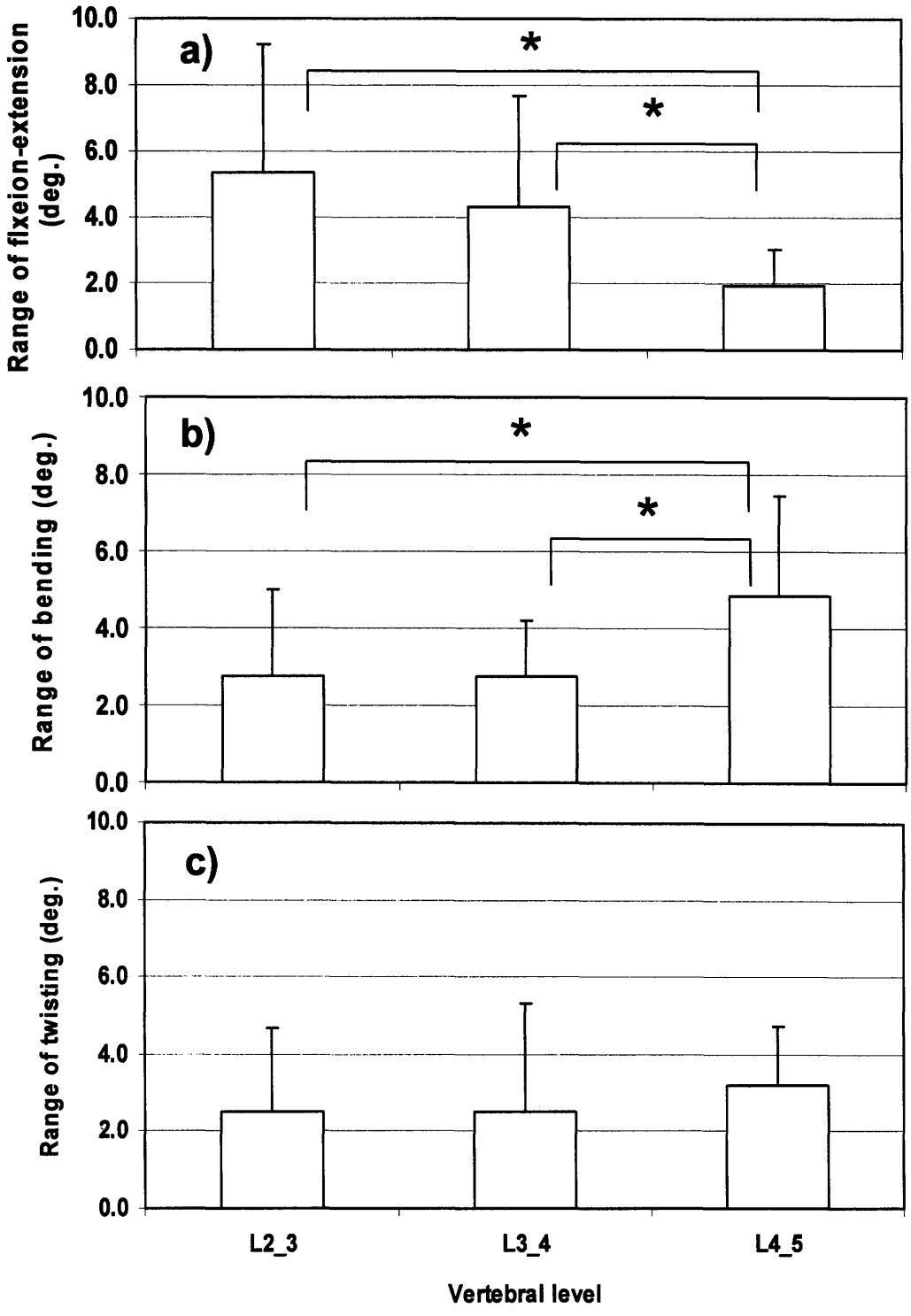

Figure 4-5: The range of motion of three vertebral levels during various physiologic activities.

4.2.2 In-vivo disc deformation

Different segment discs showed different deformation distributaries. L2-3 disc had an overall largest deformation. During standing, the anterior portion of the disc experienced average about 15% tension and the posterior part experienced -12% compressive deformation. In flexion activity, the anterior tension decreased to 10% tension while the compression at posterior portion changed to -10%. In extension, the anterior tension increases to 18% and the posterior stays the same. (**Fig. 4-6**) The left and right edge and center portion exhibited small deformation (about 0%) during these in-vivo activities. However during left/right twisting (**Fig. 4-7**) and bending (**Fig. 4-8**), the values ranged between 5% tension and compression. L3-4 disc showed a similar trend as L2-3 while the absolute deformation value is about 5% smaller. L4-5 disc showed an average 10-15% smaller absolute deformation than L2-3 in anterior and posterior portion, which resulted an opposite tension and compression deformation in certain activities for some subjects. However, the deformation increased to 10% at twisting and bending activities. Overall, these data presented a first attempt to study in-vivo disc deformation under physiologic loadings.

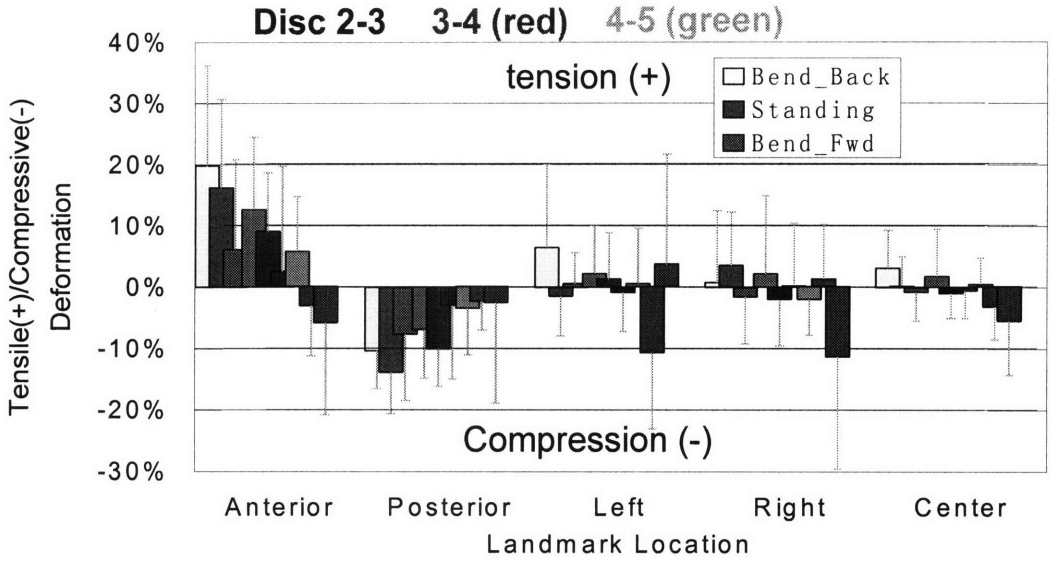

Figure 4-6: The disc deformation at different portions during flexion and extension.

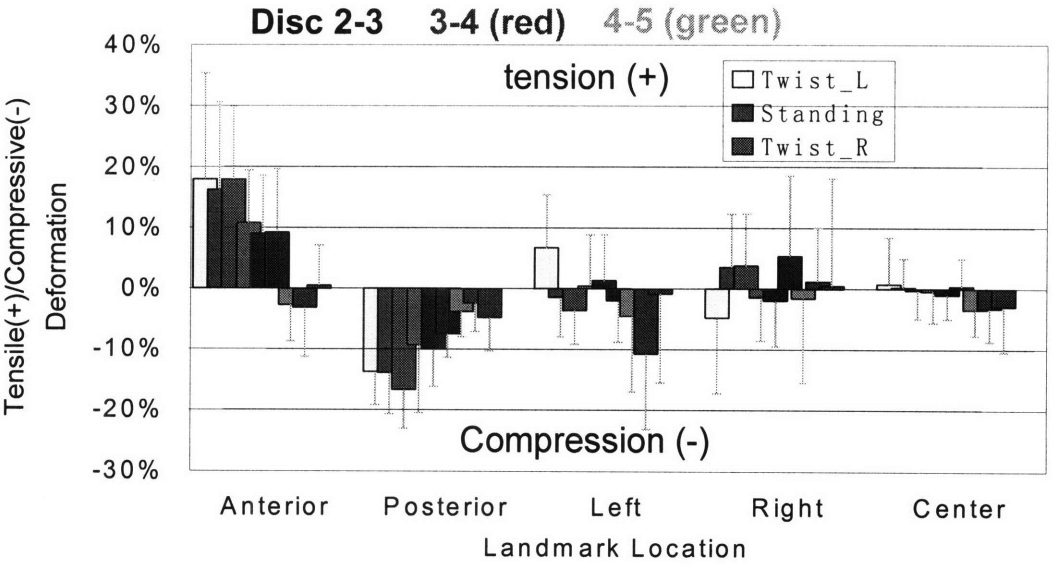

Figure 4-7: The disc deformation at different portions during left and right twist.

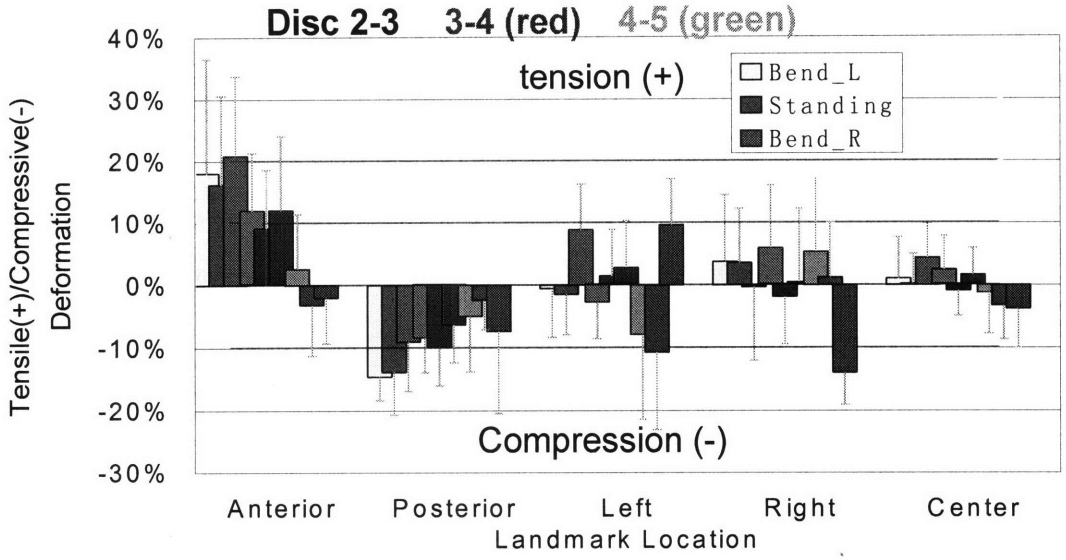

Figure 4-8: The disc deformation at different portions during left and right bend.

4.3 Discussion

Quantitative data on in-vivo vertebral motion is critical to enhance understanding of spinal pathology and to improve the current surgical treatment methods for spinal diseases. In this study, the MR combined DFIS technique was applied to measure lumbar segment motion L2-L5. The range of lumbar vertebral motion in living subjects is investigated when they performed unrestricted weightbearing activities. The data demonstrated that the upper vertebrae had larger ranges of flexion than the lower vertebrae during functional flexion-extension of the body. During the functional bending activity, the L4-5 had a larger range of left-right bending motion than both L2-3 and L3-4, while no statistical difference was observed in left-right twist among the 3 vertebral levels. Besides the primary rotations, coupled motions were found in all other DOFs. The coupled translation in left-right and anterior-posterior directions, on averaged, reached above 1 mm, while in the proximal-distal direction this remained less than 1 mm.

The data demonstrated similar ROMs compared to the literature. Pearcy and Tilbrewal [121] studied a similar twisting movement while standing and showed a range of axial rotation of approximately 2° at each vertebral level, which is similar to our findings. Haughton et al. [124] investigated lumbar twisting using MR image scan with the subject laying supine and showed an average range of axial rotation between 1 to 2° in the 3 vertebral levels. More recently, Ochia et al. [79] determined that the upper lumbar motion segments had greater amounts of axial rotation range compared to the lower segments using CT scanning. Their range of rotation was about 3-4°. Pearcy et al. found that coupled translation in left-right and anterior-posterior directions were around the range of 1 mm during primary flexion-extension motion, which are similar to our findings. More detailed comparison will be discussed in the following Chapter.

From these normal subject data, we found that disc deformation is segmental dependent and inhomogeneous. L2-3 has an overall largest deformation at the anterior with tension and posterior with compression, while L4-5 has a largest deformation at left and right portion of the disc. The center portion has small deformation around 0% during all physiologic functional activities. As far as we know, the only literature related reported an average of 4.4% height loss (compressive deformation) over the whole disc under 1000N compression axial load using MRI [110].

It is assumed that the above calculation of geometric deformation is an accurate measurement of 3D disc deformation. In the future, a 3D finite element model will be established using the disc attachment positions before and after motion as geometric boundaries to calculate the actual 3D strain distribution.

4.4 Summary

In conclusion, this Chapter used the MR combined DFIS method to investigate functional lumbar spine motion in human subjects under weightbearing conditions. The advantage of this system for spinal research is its flexibility to accommodate various functional activities. This Chapter reports data on lumbar vertebral motion ranges during 3 unrestricted body motions commonly used during clinical examinations of the spine. Vertebral motion at different levels may respond to external loads differently. The in-vivo kinematics also suggested segmental dependent and inhomogeneous disc deformation. These data may provide new insight into the in-vivo function of human spines. The method proved to be a useful tool that can be readily applied to spine study. Future study will focus on the in-vivo vertebral kinematics and disc deformation of patients with diseased discs and to analyze how surgical treatment will affect the spinal biomechanics. Future investigations will also be directed at examining the deformation of the lumbar spine segments using 3D finite element analysis while using the 6DOF kinematics determined in this study as boundary conditions.

Chapter 5

Discussion

5.1 Advantages and limitations

The study on spine biomechanics has been pursued for decades. However, due to the complex anatomy and limited technology, a quantitative understanding of kinematics and IVD deformation in the human spine under in-vivo physiologic functional activities remains elusive. In-vitro studies commonly use invasive techniques to obtain their measurements which add morbidity when applied to an in-vivo setting. Finite element studies have the obvious disadvantage of the overwhelming parameters, and the relevance remains a challenge. Finally, the in-vivo measurements obtained are limited by the apparatus and methodology. They are either not accurate enough or not able to test physiologic functional activities of everyday life.

The study investigated a MRI combined dual fluoroscopic imaging technique to study in-vivo human lumbar spine biomechanics. As newly developed, this technique exhibits several advantages compare to conventional in-vitro, finite element or even current in-vivo methods. First of all, this basic conceptual of this method is image matching, which impose minimum intervention to human body. The non-invasive characteristic is especially critical when study sensitive areas such as spine. Secondly, the method has shown sufficient accuracy and repeatability through several pilot studies on determining in-vivo human joint position and cartilage deformation [5-8]. The validation of this method for the lumbar spine has been done on Chapter 3 and a sufficient accuracy

and repeatability was obtained for effectively study spine biomechanics. Last but not the least, the experiment setting is easy to access and reproduced in clinical environment. Study subjects are free to move and perform physiologic functional activities, which provide most relevant date on the intrinsic biomechanics of the human spine. The data will provide baseline information of the relationship between abnormal in-vivo biomechanics and the mechanisms of spinal degeneration. The knowledge obtained from this study will help to establish guidelines for the improvement of current surgical techniques and implant design for the treatment of patients with varying degrees of degenerative changes, as well as provide objective functions for the development of tissue engineered biomaterials for disc degeneration repair.

There are several limitations to the current method. Even though MR model introduced minimum radiation exposure on the human subjects, the manual segmentation of spine bony outline is time consuming and tedious. The matching process is also time consuming and the accuracy and repeatability is dependent on each individual. Potential solutions are to develop automatic segmentation and automatic matching protocol in the future. However, these remain big challenging due to the intrinsic complex anatomy of vertebrae segments.

In the in-vivo human lumbar spine study presented in Chapter 4, subjects were asked to perform some maximum torso motions. Inter-subjects variation of range of motion may be a problem that will cause relatively large standard deviation of the obtained data. Regulating a standard motion is necessary for future studies, the experienced spine MDs will assist to pose the subjects. A few warm-up flexions will also be incorporated aim to minimize the inter-subject variation and enhance the statistical power of the data. In order to keep the targeted lumbar spine within the field view of the two fluoroscopes, the subject

was instructed to limit flexion to approximately 45° from a standing position. Also, only the ROM of the L2-3, L3-4 and L4-5 segments were examined during the 3 functional body motions. The in-vivo instantaneous positions of the vertebrae during dynamic motion of the body were not examined. Finally, the subjects were within the age distribution of 50 to 60 years. In future, living subjects in various age ranges should be investigated to examine the age effect on vertebral kinematics. Nevertheless, the data obtained from this study will hopefully contribute to our knowledge on physiological motion of the human lumbar vertebrae.

5.2 Comparison with Previous Studies

5.2.1 Accuracy validation of the in-vivo methods

In Chapter 3, an in-vitro experimental setup was utilized to determine the accuracy and repeatability of the MR combined DFIS technique when used to determine spinal kinematics. Repeatability was also validated using 3D positions and orientations of the in-vivo human vertebrae under four weightbearing, physiologic positions of the torso. The data indicated that the method has accuracy within 0.2 mm in determination of vertebra translations and 0.2 mm/s in translational speed. The in-vivo human spine experiment demonstrated a high repeatability of the method in determination of vertebra within 0.3 mm and 0.6° for translation and orientation.

A few pioneer studies have investigated spinal vertebral motion using CT imaging [16,23,72-74,79]. Lim et al. [80] used CT images of two cervical vertebrae to verify an Eigen vector method and revealed that the method had an accuracy of 1 mm in translation and 1° in rotation. The accuracy and repeatability of similar

imaging methods have been validated by others using phantoms composed of ceramic balls [23,79]. These investigations reported accuracy between 0.1 mm to 0.52 mm and 0.2° to 0.43° for translation and orientation, respectively. A similar phantom study using various beads has also been conducted to validate the accuracy of the dual fluoroscopic imaging method used in this study in our lab [5], where an accuracy of less than 0.08 mm was demonstrated.

However, the phantom evaluation may not represent the actual accuracy of the technique when applied to measure actual spinal segment motion when soft tissues surrounding the vertebra remain intact. Bingham et al. and Hanson et al. [5,6] revealed that the dual fluoroscopic image method, when used to study total knee arthroplasty kinematics, has an accuracy 0.3 mm in translation and 0.2° in orientation. It is unclear if the same accuracy could be retained when this technique is used to measure spine kinematics. Therefore the MR combined DFIS technique is sufficient for spine biomechanics study.

5.2.2 Spine segments range of motion

To my knowledge, no previous study has reported in-vivo vertebral motion during unrestricted functional activities in humans. Pearcy et al. [122] investigated lumbar vertebral motion during maximal flexion-extension using a biplanar radiography technique, where the pelvis and hips were limited in motion by using a rig. Their data showed similar ranges of motion for all vertebrae. The study presented in Chapter 4 found the upper levels had a larger range of flexion than the lower levels. This differing trend in flexion range may be due to two factors. First, in our testing the subject was allowed free weightbearing motion of the body. No restriction was applied to the pelvis or hips. Therefore, pelvic rotation could conceibably affect the rotation of the lumbar vertebrae. A second factor may be that we only allowed maximal flexion to approximately 45° for the upper body

which may not necessarily be maximal flexion angle of the body. While overall their coupled range of translation was found to be similar in magnitude to our data, the coupled rotation data was lower in magnitude than our data. The differences between the two studies emphasize the importance of functional activities and motion pattern when investigating the vertebral kinematics.

Pearcy et al. [121] also investigated left-right bending rotation motion (also referred to as lateral bending rotation) of living subjects using their biplanar radiography technique. Overall, they found larger ranges of lateral bending rotation than we did in our studies. They also reported larger bending ranges in the upper segments compared to the lower levels of the vertebrae. In my data, however, I found that the lower level L4-5 had a larger range of bending rotation than the upper two levels. Similarly to the flexion-extension motion, the lateral bending motion was also affected by the motion of the pelvis and hips. In my study, an unrestricted lateral bending was performed by all subjects. It might be difficult to directly compare the results between different studies given that the functional activities were inconsistent.

There are several studies that have investigated left and right twisting (also referred to as axial rotation in literature) of lumbar spine in living subjects under various conditions [79,121,122,124]. For example, Pearcy and Tilbrewal [121] studied a similar twisting movement while standing and showed a range of axial rotation of approximately 2° at each vertebral level, which is similar to my findings. Haughton et al. [124] investigated lumbar twisting using MR image scan while the subject laying supine and showed an average range of axial rotation between 1 to 2° in the 3 vertebral levels. Their measurement was carried by rotation of the lower body ±8° to examine the rotation range of the vertebrae. More recently, Ochia et al. [79] determined that the upper lumbar motion segments had greater

amounts of axial rotation range compared to the lower segments when the upper body was passively rotated to ±50° in supine position and CT scanned and their range of rotation was almost twice that found in the above mentioned studies.

These large discrepancies in vertebral rotation data could be explained by the various functional activities used in these studies that were caused by different experimental setups. Pearcy and Tibrewal studied similar active weightbearing axial rotations compared with my study. However, both Haughton et al. [124] and Ochia et al. [79] studied passive axial rotation of the body in supine position. Haughton et al. rotated the subject's hip ±8° to investigate the lumber spine rotation while Ochia et al. rotated the upper body ±50° to measure the lumbar spine rotation. In both of these two studies, however, the spine was not under weightbearing conditions. A quantitative comparison between these studies might be difficult and a comparison of lumbar vertebral motions has to consider of the different functional activities that were present among these studies.

Few studies have gone further to investigate coupled vertebral motions with the primary rotations [79,122]. Pearcy et al. found that coupled translation in left-right and anterior-posterior directions were around the range of 1 mm during primary flexion-extension motion which is similar to my findings. However, the accuracy of their system was around 1 mm [121]. Their coupled motion in left-right bending and axial rotation were also similar to mys. During primary axial rotation, Ochia et al. found that the coupled range of translation in left-right direction was over 8 mm at L2-3, over 4 mm at L3-4 and over 1 mm at L4-5 levels. These are larger than those measured from my study during standing weightbearing axial rotation. Their coupled translation in anterior-posterior and proximal-distal directions were lower than those reported in my study. These comparisons indicated again that the coupled vertebral motions are also loading dependent.

In conclusion, the study in Chapter 4 used MR combined DFIS as a first attempt to investigate functional lumbar spine motion in human subjects under weightbearing conditions. Compare to literature, the advantage of this system for spinal research is its flexibility to accommodate various functional activities. Data was reported on lumbar vertebral motion ranges during 3 unrestricted body motions commonly used during clinical examinations of the spine. Vertebral motion at different levels may respond to external loads differently. These data may provide new insight into the in-vivo function of human spines.

5.2.3 In-vivo disc deformation

Due to the limitation of technique, in-vivo human disc deformation research attempts have primarily concentrated on the measurement of strain and the evaluation of nuclear migration using imaging technique such as MRI. The details was discussed in Chapter one. Utilizing MR combined DFIS image matching technology, the in-vivo disc deformation was determined under various physiologic activities. Quantified data was obtained as a potential to study disc degeneration related LBP and to improve surgical treatment such as spinal fusion and total disc replacement. To my knowledge, the only related research is conducted by O'Connell et al [110]. They proposed an in-vitro study to a potential in-vivo MRI method to determine disc strains non-invasively in axial compression. MR images were acquired before and during application of a 1000 N axial compression. Two-dimensional internal displacements, average strains, and the location and direction of peak strains were calculated using texture correlation, a pattern matching algorithm. Their study reported an average of 4.4% height loss (compressive deformation) over the whole disc. The study in Chapter 4 using our image matching method reported deformation of various portions (anterior, posterior, left, right and center) of disc levels L2-3, L3-4 and L4-5 from various

physiologic functional activities. Inhomogeneous deformation as well as segmental dependent characters was found. Thus, the MR combined DFIS method showed has a promising application on future disc deformation studies.

5.3 CT versus MR models for combined DFIS study

In Chapter 2 the spine specimen was imaged using both CT and MR. Since CT images have been used by various researchers [16,24,72-78], the CT imaging model was used as a comparison with the MR image-based model. The comparison was carried out by two parts. First the geometry of the two models was compared using the iterative closest point (ICP) method [114]. About 4000 points were picked from both vertebral body models. The average difference between the two mesh models was calculated to be 0.07±1.1 mm when mapping MR model to CT model. Then in the validation test using the MTS machine as a gold standard, both the CT and MR models resulted in similar accuracy with the CT model having on average a slightly better accuracy. This difference was not found to be statistically significant. Both models also showed similar accuracy in the determination of the speed of spinal motion. In the repeatability test using manual dynamic flexion/extension of the spinal segment, both the CT and MR models also showed a similar reproducibility in determination of 6DOF spinal positions.

Even though both the CT and MR models had similar accuracy and repeatability results, there is one inherent benefit of using CT imaging for the application of our technique. CT images may facilitate automatic segmentation with commercially available software. In contrast, automatic segmentation for MR models is currently time consuming. However, when measuring vertebral kinematics in human subjects, the dosage of radiation to which the subjects are exposed when utilizing CT imaging may present an ethical concern for the safety

of the individuals being tested. Alternatively, MR model provide us with greater visualization of the ligamentous components surrounding the lumbar vertebra as well as their relation to relevant neurologic structures in this area. Therefore, in order to minimize the risk to the subjects involved in this study and to enhance our ability to look at the soft-tissue structures of the lumbar spine for further study on pathology, MR imaging based model was selected to be used exclusively in order to capture the 3D geometry of the lumbar spine for the human subjects.

5.4 Future Work

In the study, the MR combined DFIS technique showed adequate accuracy and effective application for study in-vivo human spine biomechanics such as range of motion and disc deformation non-invasively. This technique can be carried out on study various spine studies. The future work may consist of three aspects: the perfection of the imaging technology, the improvement of data analysis and the vastitude of application.

With the advance in medical image techniques, we anticipate that there will be a progressive improvement in our ability to obtain fluoroscopic and MR images that were not available at the time of this study. Research will be conducted on the MR sequences aiming at different part of spine osseous, surrounding soft tissues or joints to continuously adjust the protocol during the ongoing studies in order to improve the resolution of the focused anatomic features. We therefore anticipate that with further refinement of our technique, coupled with technological advancements in fluoroscopic and MR imaging modalities, the accuracy and reliability of our technique will be improved. As mentioned before, the current image matching technique employees manual segmentation of the MRI model and manual matching of the model to fluoroscopic images. The process is very time

consuming and the error was introduced from variability of each individual researcher. In literature, automatic segmentation is feasible on human joint MRI through various edge detection methods. Automatic or semi automatic method should be developed on human spine MRI model. On the other hand, the optimal solution would be to develop an automatic program. However, the naturally complex anatomies of spine segments are hard to be matched automatically. Knowledge of the anatomy and experience of matching are very important. So a standardized teaching and learning protocol should be developed on the matching process to minimize any variation and enhance the statistical power of the data.

In the disc deformation study presented in Chapter 4, the geometric deformations of five pairs of points are studied to represent the deformation of the whole disc. However this analysis can be improved by introducing stress strain tensor to look at the 3D deformation throughout the whole disc. Finite element models (FEM) have been applied to understand the relationships between the biomechanical performance of the disc and disc degeneration. Nonlinearity of the material and geometry has been considered in the model [58-60]. Viscoelasticity and fiber-reinforced annulus fibrosus (AF) was introduced [61-63]. Recently, a popular poroelastic material behavior has been introduced to FEM to consider fluid flow of the disc [64-68]. Regional poroelastic material properties and strain-dependent permeability and porosity has also been investigated [69,70]. Elasticity, poroelasticity and other material properties from these spine studies should be incorporated and finally a finite element model should be utilized to fully analysis and understand the in-vivo disc deformation based on the 6DOF kinematics from image matching technique.

It has been reported that 75% of all adults will experience LBP secondary to degenerative changes in the lumbar spine at some point in their lifetime [3,4]. The

total cost of LBP in the United States exceeds $100 billion per year [127]. Altered vertebral kinematics has been assumed to be a critical factor leading to disc degeneration related LBP. To fully understand this problem, studies on normal subjects as well as LBP patients are required. The current investigation quantifies the in-vivo 6DOF kinematics of the normal lumbar spine. A thorough pilot study has been performed to validate and to investigate the measurement of in-vivo vertebral kinematics and disc deformation. Early stage of disc degeneration without symptom was observed in the normal subjects. In this study, we exclude the subjects with any disc degeneration to make the study focused. However, these data will provide a foundation for future studies on the relationship among DDD, mechanism causes LBP and altered kinematics and disc deformation. Subjects with early disc degeneration will be investigated in future studies. LBP patients before and after surgical treatment will be included in the study in the future. The patients will be sequentially recruited from the spine service of the Massachusetts General Hospital. These are patients who visit our clinic because of lower back pain attributed to disc degeneration and are scheduled to undergo fusion surgery between the L4 and S1 levels. We aim to focus our research on the superior adjacent levels from L1 to L5. A review of our previous patient data indicates that there are approximately 100 patients seen annually in our clinic who will meet our criteria. The image matching method will also be applied on patients after surgery and long-term follow up will be conducted. In chapter 4 the study only investigates the subjects during designed physiologic functional activities such as flexion, bending and twisting. However, DDD and LBP are often related to weight lifting activities. And the study on dynamic gaiting will help greatly to restore normal function of spine segments. Further research may be carried on weight lifting and dynamic gating activities.

5.5 Summary

This study validated the MR combined DFIS image matching method using both in-vitro and in-vivo experiment setup. The method was used to measure the in-vivo 6DOF lumbar vertebral kinematics and disc deformation of normal subjects during various torso motions of daily activities. These will sever as base line research for the future quantitatively investigation of in-vivo lumbar spine kinematics and IVD deformation of normal human subjects as well as in patients with LBP both before and after fusion surgery. The long-term goal is to delineate the biomechanical mechanisms of LBP and to improve our current surgical modalities. The newly developed non-invasive imaging technique should provide important information on the intrinsic biomechanics of the human spine. The data will provide valuable information on spinal kinematics. This research is a first attempt to study kinematics and disc deformation in normal subjects under in-vivo physiologic functional activities. It will provide baseline information of the relationship between abnormal in-vivo biomechanics and the mechanisms of spinal degeneration. The knowledge obtained from this study will help to establish guidelines for the improvement of current surgical techniques and implant design for the treatment of patients with varying degrees of DDD, as well as provide objective functions for the development of tissue engineered biomaterials for disc degeneration repair.

References

1. Smedley J, Inskip H, Cooper C, et al. Natural history of low back pain. A longitudinal study in nurses. Spine 1998;23:2422-6.

2. Heliovaara M, Sievers K, Impivaara O, et al. Descriptive epidemiology and public health aspects of low back pain. Ann Med 1989;21:327-33.

3. Jandric S, Antic B. [Low back pain and degenerative disc disease]. Med Pregl 2006;59:456-61.

4. Kosharskyy B, Rozen D. [Discogenic low back pain. Minimally invasive interventional therapies]. Anasthesiol Intensivmed Notfallmed Schmerzther 2007;42:262-7.

5. Bingham J, Li G. An optimized image matching method for determining in-vivo TKA kinematics with a dual-orthogonal fluoroscopic imaging system. J Biomech Eng 2006;128:588-95.

6. Hanson GR, Suggs JF, Freiberg AA, et al. Investigation of in vivo 6DOF total knee arthoplasty kinematics using a dual orthogonal fluoroscopic system. J Orthop Res 2006;24:974-81.

7. Li G, Wan L, Kozanek M. Determination of real-time in-vivo cartilage contact deformation in the ankle joint. J Biomech 2008;41:128-36.

8. Bingham J, Papannagari R, Gross C, et al. In-vivo Cartilage Contact Deformation in the Healthy Human Tibiofemoral Joint J Orthop Res 2008.

9. Wang S, Wood K, Li G. Inhomogenerous Deformation of the Intervertebral Disc under In-vivo Weightbearing Conditions. 54th Annual Meeting of the Orthopaedic Research Society. San Francisco, 2008.

10. Wan L, de Asla RJ, Rubash HE, et al. Determination of in-vivo articular cartilage contact areas of human talocrural joint under weightbearing conditions. Osteoarthritis Cartilage 2006;14:1294-301.

11. Defrate LE, van der Ven A, Boyer PJ, et al. The measurement of the variation in the surface strains of Achilles tendon grafts using imaging techniques. J Biomech 2006;39:399-405.

12. Wang S, Li G, Passias P, et al. Measurement of Vertebral Kinematics Using Non-invasive Image Matching Method - Validation and Application. Spine 2008.

13. de Asla RJ, Wan L, Rubash HE, et al. Six DOF in vivo kinematics of the

ankle joint complex: Application of a combined dual-orthogonal fluoroscopic and magnetic resonance imaging technique. J Orthop Res 2006;24:1019-27.

14. Boyer PJ, Massimini DF, Gill TJ, et al. In-vivo Articular Cartilage Contact at the Glenohumeral Joint. J Orthop Res 2008.

15. Auerbach JD, Wills BP, McIntosh TC, et al. Evaluation of spinal kinematics following lumbar total disc replacement and circumferential fusion using in vivo fluoroscopy. Spine 2007;32:527-36.

16. Siddiqui M, Karadimas E, Nicol M, et al. Effects of X-STOP device on sagittal lumbar spine kinematics in spinal stenosis. J Spinal Disord Tech 2006;19:328-33.

17. Wong KW, Luk KD, Leong JC, et al. Continuous dynamic spinal motion analysis. Spine 2006;31:414-9.

18. Kotani Y, Abumi K, Shikinami Y, et al. Artificial intervertebral disc replacement using bioactive three-dimensional fabric: design, development, and preliminary animal study. Spine 2002;27:929-35; discussion 35-6.

19. Zhu Q, Larson CR, Sjovold SG, et al. Biomechanical evaluation of the Total Facet Arthroplasty System: 3-dimensional kinematics. Spine 2007;32:55-62.

20. Kettler A, Marin F, Sattelmayer G, et al. Finite helical axes of motion are a useful tool to describe the three-dimensional in vitro kinematics of the intact, injured and stabilised spine. Eur Spine J 2004;13:553-9.

21. Miura T, Panjabi MM, Cripton PA. A method to simulate in vivo cervical spine kinematics using in vitro compressive preload. Spine 2002;27:43-8.

22. SariAli el H, Lemaire JP, Pascal-Mousselard H, et al. In vivo study of the kinematics in axial rotation of the lumbar spine after total intervertebral disc replacement: long-term results: a 10-14 years follow up evaluation. Eur Spine J 2006;15:1501-10.

23. Ishii T, Mukai Y, Hosono N, et al. Kinematics of the upper cervical spine in rotation: in vivo three-dimensional analysis. Spine 2004;29:E139-44.

24. Lindsey DP, Swanson KE, Fuchs P, et al. The effects of an interspinous implant on the kinematics of the instrumented and adjacent levels in the lumbar spine. Spine 2003;28:2192-7.

25. Dickman CA, Crawford NR, Tominaga T, et al. Morphology and kinematics of the baboon upper cervical spine. A model of the atlantoaxial complex. Spine 1994;19:2518-23.

26. Lee S, Harris KG, Nassif J, et al. In vivo kinematics of the cervical spine. Part I: Development of a roentgen stereophotogrammetric technique using metallic markers and assessment of its accuracy. J Spinal Disord 1993;6:522-34.

27. Goel VK, Clark CR, McGowan D, et al. An in-vitro study of the kinematics of the normal, injured and stabilized cervical spine. J Biomech 1984;17:363-76.

28. Fujiwara A, Lim TH, An HS, et al. The effect of disc degeneration and facet joint osteoarthritis on the segmental flexibility of the lumbar spine. Spine 2000;25:3036-44.

29. Gilchrist CL, Chen J, Richardson WJ, et al. Functional integrin subunits regulating cell-matrix interactions in the intervertebral disc. J Orthop Res 2007;25:829-40.

30. Korecki CL, MacLean JJ, Iatridis JC. Characterization of an in vitro intervertebral disc organ culture system. Eur Spine J 2007;16:1029-37.

31. Lee CR, Iatridis JC, Poveda L, et al. In vitro organ culture of the bovine intervertebral disc: effects of vertebral endplate and potential for mechanobiology studies. Spine 2006;31:515-22.

32. Jackson AR, Yuan TY, Huang CY, et al. Effect of compression and anisotropy on the diffusion of glucose in annulus fibrosus. Spine 2008;33:1-7.

33. Miyamoto H, Doita M, Nishida K, et al. Effects of cyclic mechanical stress on the production of inflammatory agents by nucleus pulposus and anulus fibrosus derived cells in vitro. Spine 2006;31:4-9.

34. Reza AT, Nicoll SB. Hydrostatic pressure differentially regulates outer and inner annulus fibrosus cell matrix production in 3D scaffolds. Ann Biomed Eng 2008;36:204-13.

35. Haschtmann D, Stoyanov JV, Ferguson SJ. Influence of diurnal hyperosmotic loading on the metabolism and matrix gene expression of a whole-organ intervertebral disc model. J Orthop Res 2006;24:1957-66.

36. Handa T, Ishihara H, Ohshima H, et al. Effects of hydrostatic pressure on matrix synthesis and matrix metalloproteinase production in the human lumbar intervertebral disc. Spine 1997;22:1085-91.

37. van Deursen DL, Snijders CJ, Kingma I, et al. In vitro torsion-induced stress distribution changes in porcine intervertebral discs. Spine 2001;26:2582-6.

38. Iatridis JC, Setton LA, Foster RJ, et al. Degeneration affects the anisotropic and nonlinear behaviors of human anulus fibrosus in compression. J Biomech

1998;31:535-44.

39. Iatridis JC, MaClean JJ, Ryan DA. Mechanical damage to the intervertebral disc annulus fibrosus subjected to tensile loading. J Biomech 2005;38:557-65.

40. Hedman TP, Fernie GR. Mechanical response of the lumbar spine to seated postural loads. Spine 1997;22:734-43.

41. Frei H, Oxland TR, Nolte LP. Thoracolumbar spine mechanics contrasted under compression and shear loading. J Orthop Res 2002;20:1333-8.

42. Lu WW, Luk KD, Holmes AD, et al. Pure shear properties of lumbar spinal joints and the effect of tissue sectioning on load sharing. Spine 2005;30:E204-9.

43. Ranu HS. Multipoint determination of pressure-volume curves in human intervertebral discs. Ann Rheum Dis 1993;52:142-6.

44. Bono CM, Lee CK. Critical analysis of trends in fusion for degenerative disc disease over the past 20 years: influence of technique on fusion rate and clinical outcome. Spine 2004;29:455-63; discussion Z5.

45. Adams MA, Freeman BJ, Morrison HP, et al. Mechanical initiation of intervertebral disc degeneration. Spine 2000;25:1625-36.

46. Stokes IA. Bulging of lumbar intervertebral discs: non-contacting measurements of anatomical specimens. J Spinal Disord 1988;1:189-93.

47. Heggeness MH, Doherty BJ. Discography causes end plate deflection. Spine 1993;18:1050-3.

48. Costi JJ, Stokes IA, Gardner-Morse M, et al. Direct measurement of intervertebral disc maximum shear strain in six degrees of freedom: motions that place disc tissue at risk of injury. J Biomech 2007;40:2457-66.

49. Kusaka Y, Nakajima S, Uemura O, et al. Intradiscal solid phase displacement as a determinant of the centripetal fluid shift in the loaded intervertebral disc. Spine 2001;26:E174-81.

50. Seroussi RE, Krag MH, Muller DL, et al. Internal deformations of intact and denucleated human lumbar discs subjected to compression, flexion, and extension loads. J Orthop Res 1989;7:122-31.

51. Tsantrizos A, Ito K, Aebi M, et al. Internal strains in healthy and degenerated lumbar intervertebral discs. Spine 2005;30:2129-37.

52. Stokes IA. Surface strain on human intervertebral discs. J Orthop Res

1987;5:348-55.

53. Meakin JR, Redpath TW, Hukins DW. The effect of partial removal of the nucleus pulposus from the intervertebral disc on the response of the human annulus fibrosus to compression. Clin Biomech (Bristol, Avon) 2001;16:121-8.

54. Bradford DS, Oegema TR, Jr., Cooper KM, et al. Chymopapain, chemonucleolysis, and nucleus pulposus regeneration. A biochemical and biomechanical study. Spine 1984;9:135-47.

55. Goel VK, Goyal S, Clark C, et al. Kinematics of the whole lumbar spine. Effect of discectomy. Spine 1985;10:543-54.

56. Panjabi MM, Krag MH, Chung TQ. Effects of disc injury on mechanical behavior of the human spine. Spine 1984;9:707-13.

57. Lu DS, Shono Y, Oda I, et al. Effects of chondroitinase ABC and chymopapain on spinal motion segment biomechanics. An in vivo biomechanical, radiologic, and histologic canine study. Spine 1997;22:1828-34; discussion 34-5.

58. Kim YE, Goel VK, Weinstein JN, et al. Effect of disc degeneration at one level on the adjacent level in axial mode. Spine 1991;16:331-5.

59. Kurowski P, Kubo A. The relationship of degeneration of the intervertebral disc to mechanical loading conditions on lumbar vertebrae. Spine 1986;11:726-31.

60. Natarajan RN, Ke JH, Andersson GB. A model to study the disc degeneration process. Spine 1994;19:259-65.

61. Lu YM, Hutton WC, Gharpuray VM. Do bending, twisting, and diurnal fluid changes in the disc affect the propensity to prolapse? A viscoelastic finite element model. Spine 1996;21:2570-9.

62. Goel VK, Monroe BT, Gilbertson LG, et al. Interlaminar shear stresses and laminae separation in a disc. Finite element analysis of the L3-L4 motion segment subjected to axial compressive loads. Spine 1995;20:689-98.

63. Kim Y. Prediction of peripheral tears in the anulus of the intervertebral disc. Spine 2000;25:1771-4.

64. Wu JS, Chen JH. Clarification of the mechanical behaviour of spinal motion segments through a three-dimensional poroelastic mixed finite element model. Med Eng Phys 1996;18:215-24.

65. Argoubi M, Shirazi-Adl A. Poroelastic creep response analysis of a lumbar motion segment in compression. J Biomech 1996;29:1331-9.

66. Silva P, Crozier S, Veidt M, et al. An experimental and finite element poroelastic creep response analysis of an intervertebral hydrogel disc model in axial compression. J Mater Sci Mater Med 2005;16:663-9.

67. Lee CK, Kim YE, Lee CS, et al. Impact response of the intervertebral disc in a finite-element model. Spine 2000;25:2431-9.

68. Cheung JT, Zhang M, Chow DH. Biomechanical responses of the intervertebral joints to static and vibrational loading: a finite element study. Clin Biomech (Bristol, Avon) 2003;18:790-9.

69. Williams JR, Natarajan RN, Andersson GB. Inclusion of regional poroelastic material properties better predicts biomechanical behavior of lumbar discs subjected to dynamic loading. J Biomech 2007;40:1981-7.

70. Natarajan RN, Williams JR, Andersson GB. Modeling changes in intervertebral disc mechanics with degeneration. J Bone Joint Surg Am 2006;88 Suppl 2:36-40.

71. Lee KK, Teo EC. Poroelastic analysis of lumbar spinal stability in combined compression and anterior shear. J Spinal Disord Tech 2004;17:429-38.

72. Si-Hoe KM, Teoh SH, Teo J. Radio-translucent 3-axis mechanical testing rig for the spine in micro-CT. J Biomech Eng 2006;128:957-64.

73. Simon S, Davis M, Odhner D, et al. CT imaging techniques for describing motions of the cervicothoracic junction and cervical spine during flexion, extension, and cervical traction. Spine 2006;31:44-50.

74. Gocen S, Havitcioglu H, Alici E. A new method to measure vertebral rotation from CT scans. Eur Spine J 1999;8:261-5.

75. Martin H, Werner J, Andresen R, et al. Noninvasive assessment of stiffness and failure load of human vertebrae from CT-data. Biomed Tech (Berl) 1998;43:82-8.

76. Rho JY, Hobatho MC, Ashman RB. Relations of mechanical properties to density and CT numbers in human bone. Med Eng Phys 1995;17:347-55.

77. Moga PJ, Erig M, Chaffin DB, et al. Torso muscle moment arms at intervertebral levels T10 through L5 from CT scans on eleven male and eight female subjects. Spine 1993;18:2305-9.

78. Breau C, Shirazi-Adl A, de Guise J. Reconstruction of a human ligamentous lumbar spine using CT images--a three-dimensional finite element mesh generation. Ann Biomed Eng 1991;19:291-302.

79. Ochia RS, Inoue N, Renner SM, et al. Three-dimensional in vivo measurement of lumbar spine segmental motion. Spine 2006;31:2073-8.

80. Lim TH, Eck JC, An HS, et al. A noninvasive, three-dimensional spinal motion analysis method. Spine 1997;22:1996-2000.

81. Kulig K, Powers CM, Landel RF, et al. Segmental lumbar mobility in individuals with low back pain: in vivo assessment during manual and self-imposed motion using dynamic MRI. BMC Musculoskelet Disord 2007;8:8.

82. Urban JP, Winlove CP. Pathophysiology of the intervertebral disc and the challenges for MRI. J Magn Reson Imaging 2007;25:419-32.

83. Karadimas EJ, Siddiqui M, Smith FW, et al. Positional MRI changes in supine versus sitting postures in patients with degenerative lumbar spine. J Spinal Disord Tech 2006;19:495-500.

84. Fazey PJ, Song S, Monsas S, et al. An MRI investigation of intervertebral disc deformation in response to torsion. Clin Biomech (Bristol, Avon) 2006;21:538-42.

85. Sairyo K, Katoh S, Takata Y, et al. MRI signal changes of the pedicle as an indicator for early diagnosis of spondylolysis in children and adolescents: a clinical and biomechanical study. Spine 2006;31:206-11.

86. Kaale BR, Krakenes J, Albrektsen G, et al. Head position and impact direction in whiplash injuries: associations with MRI-verified lesions of ligaments and membranes in the upper cervical spine. J Neurotrauma 2005;22:1294-302.

87. Perie D, Iatridis JC, Demers CN, et al. Assessment of compressive modulus, hydraulic permeability and matrix content of trypsin-treated nucleus pulposus using quantitative MRI. J Biomech 2006;39:1392-400.

88. Jinkins JR, Dworkin JS, Damadian RV. Upright, weight-bearing, dynamic-kinetic MRI of the spine: initial results. Eur Radiol 2005;15:1815-25.

89. Kourtis D, Magnusson ML, Smith F, et al. Spine height and disc height changes as the effect of hyperextension using stadiometry and MRI. Iowa Orthop J 2004;24:65-71.

90. Gilchrist CL, Xia JQ, Setton LA, et al. High-resolution determination of soft tissue deformations using MRI and first-order texture correlation. IEEE Trans Med Imaging 2004;23:546-53.

91. Kulig K, Landel R, Powers CM. Assessment of lumbar spine kinematics using dynamic MRI: a proposed mechanism of sagittal plane motion induced by

manual posterior-to-anterior mobilization. J Orthop Sports Phys Ther 2004;34:57-64.

92. Jinkins JR, Dworkin J. Proceedings of the State-of-the-Art Symposium on Diagnostic and Interventional Radiology of the Spine, Antwerp, September 7, 2002 (Part two). Upright, weight-bearing, dynamic-kinetic MRI of the spine: pMRI/kMRI. Jbr-Btr 2003;86:286-93.

93. Manenti G, Liccardo G, Sergiacomi G, et al. Axial loading MRI of the lumbar spine. In Vivo 2003;17:413-20.

94. Saifuddin A, Blease S, MacSweeney E. Axial loaded MRI of the lumbar spine. Clin Radiol 2003;58:661-71.

95. Miyati T, Mase M, Banno T, et al. Frequency analyses of CSF flow on cine MRI in normal pressure hydrocephalus. Eur Radiol 2003;13:1019-24.

96. Hutton WC, Malko JA, Fajman WA. Lumbar disc volume measured by MRI: effects of bed rest, horizontal exercise, and vertical loading. Aviat Space Environ Med 2003;74:73-8.

97. McGregor AH, Anderton L, Gedroyc WM, et al. The use of interventional open MRI to assess the kinematics of the lumbar spine in patients with spondylolisthesis. Spine 2002;27:1582-6.

98. Vitzthum HE, Konig A, Seifert V. Dynamic examination of the lumbar spine by using vertical, open magnetic resonance imaging. J Neurosurg 2000;93:58-64.

99. Breen AC, Allen R, Morris A. Spine kinematics: a digital videofluoroscopic technique. J Biomed Eng 1989;11:224-8.

100. Harvey SB, Hukins DW. Measurement of lumbar spinal flexion-extension kinematics from lateral radiographs: simulation of the effects of out-of-plane movement and errors in reference point placement. Med Eng Phys 1998;20:403-9.

101. Van Herp G, Rowe P, Salter P, et al. Three-dimensional lumbar spinal kinematics: a study of range of movement in 100 healthy subjects aged 20 to 60+ years. Rheumatology (Oxford) 2000;39:1337-40.

102. McGregor AH, Patankar ZS, Bull AM. Spinal kinematics in elite oarswomen during a routine physiological "step test". Med Sci Sports Exerc 2005;37:1014-20.

103. Burnett AF, Cornelius MW, Dankaerts W, et al. Spinal kinematics and trunk muscle activity in cyclists: a comparison between healthy controls and non-

specific chronic low back pain subjects-a pilot investigation. Man Ther 2004;9:211-9.

104. Holt PJ, Bull AM, Cashman PM, et al. Kinematics of spinal motion during prolonged rowing. Int J Sports Med 2003;24:597-602.

105. Steffen T, Rubin RK, Baramki HG, et al. A new technique for measuring lumbar segmental motion in vivo. Method, accuracy, and preliminary results. Spine 1997;22:156-66.

106. Bull AM, McGregor AH. Measuring spinal motion in rowers: the use of an electromagnetic device. Clin Biomech (Bristol, Avon) 2000;15:772-6.

107. Glazer PA, Heilmann MR, Lotz JC, et al. Use of electromagnetic fields in a spinal fusion. A rabbit model. Spine 1997;22:2351-6.

108. Ito M, Fay LA, Ito Y, et al. The effect of pulsed electromagnetic fields on instrumented posterolateral spinal fusion and device-related stress shielding. Spine 1997;22:382-8.

109. Brault JS, Driscoll DM, Laakso LL, et al. Quantification of lumbar intradiscal deformation during flexion and extension, by mathematical analysis of magnetic resonance imaging pixel intensity profiles. Spine 1997;22:2066-72.

110. O'Connell GD, Johannessen W, Vresilovic EJ, et al. Human Internal Disc Strains in Axial Compression Measured Noninvasively Using Magnetic Resonance Imaging. Spine 2007;32.

111. Kurutz M. In vivo age- and sex-related creep of human lumbar motion segments and discs in pure centric tension. J Biomech 2006;39:1180-90.

112. Li G, DeFrate LE, Park SE, et al. In vivo articular cartilage contact kinematics of the knee: an investigation using dual-orthogonal fluoroscopy and magnetic resonance image-based computer models. Am J Sports Med 2005;33:102-7.

113. Canny J. A computational approach to edge detection. IEEE Transactions on Pattern Analysis and Machine Intelligence 1986;8:679-98.

114. Ge Y, Maurer C, Fitzpatrick J. Surface-based 3-D image registration using the iterative closest point algorithm with a closest point transform. Medical Imaging: Image processing 1996;2710:358?67.

115. Gronenschild E. The accuracy and reproducibility of a global method to correct for geometric image distortion in the x-ray imaging chain. Med Phys 1997;24:1875-88.

116. Wilke HJ, Kettler A, Wenger KH, et al. Anatomy of the sheep spine and its comparison to the human spine. Anat Rec 1997;247:542-55.

117. Panjabi MM, White AA, 3rd. Basic biomechanics of the spine. Neurosurgery 1980;7:76-93.

118. Panjabi MM, Takata K, Goel VK. Kinematics of lumbar intervertebral foramen. Spine 1983;8:348-57.

119. Qiu TX, Teo EC, Lee KK, et al. Kinematics of the thoracic T10-T11 motion segment: locus of instantaneous axes of rotation in flexion and extension. J Spinal Disord Tech 2004;17:140-6.

120. Lee SW, Wong KW, Chan MK, et al. Development and validation of a new technique for assessing lumbar spine motion. Spine 2002;27:E215-20.

121. Pearcy MJ, Tibrewal SB. Axial rotation and lateral bending in the normal lumbar spine measured by three-dimensional radiography. Spine 1984;9:582-7.

122. Pearcy MJ. Stereo radiography of lumbar spine motion. Acta Orthop Scand Suppl 1985;212:1-45.

123. Fujii R, Sakaura H, Mukai Y, et al. Kinematics of the lumbar spine in trunk rotation: in vivo three-dimensional analysis using magnetic resonance imaging. Eur Spine J 2007.

124. Haughton VM, Rogers B, Meyerand ME, et al. Measuring the axial rotation of lumbar vertebrae in vivo with MR imaging. AJNR Am J Neuroradiol 2002;23:1110-6.

125. Blankenbaker DG, Haughton VM, Rogers BP, et al. Axial rotation of the lumbar spinal motion segments correlated with concordant pain on discography: a preliminary study. AJR Am J Roentgenol 2006;186:795-9.

126. Ochia RS, Inoue N, Takatori R, et al. In vivo measurements of lumbar segmental motion during axial rotation in asymptomatic and chronic low back pain male subjects. Spine 2007;32:1394-9.

127. Katz JN. Lumbar disc disorders and low-back pain: socioeconomic factors and consequences. J Bone Joint Surg Am 2006;88 Suppl 2:21-4.